Sensors and Actuators A 331 (2021) 112743

Contents lists available at ScienceDirect

Sensors and Actuators A: Physical

journal homepage: www.elsevier.com/locate/sna

Review

A review on vibration-based piezoelectric energy harvesting from the aspect of compliant mechanisms

Haitong Liang[a,b], Guangbo Hao[a,b,*], Oskar Z. Olszewski[a,*]

[a] Tyndall National Institute, University College Cork, Cork, Ireland
[b] School of Engineering and Architecture-Electrical and Electronic Engineering, University College Cork, Cork, Ireland

ARTICLE INFO

Article history:
Received 23 September 2020
Received in revised form 10 March 2021
Accepted 2 April 2021
Available online 6 April 2021

Keywords:
Piezoelectric energy harvesting
Compliant mechanism
Mechanical structures
MEMS
Normalized Power Density

ABSTRACT

Piezoelectric energy harvesters (PEHs) promote the construction of a smarter world through powering electric devices with energy scavenged from environmental vibrations by means of piezoelectric effect. To enable the piezoelectric effect, piezoelectric materials are usually attached to mechanical structures (e.g. flexible beams) that can deform due to mechanical vibration and produce strain in piezoelectric material. The mechanical structure for energy harvesting in nature is a Compliant Mechanism (CM). A large variety of structural solutions have been proposed aiming to expend the working frequency range and maximizing the energy output of PEHs. To advance PEHs, a comprehensive review on existing structural solutions and materials is necessary. According to structural characteristics of current PEHs from the aspect of CMs, designs in state of the art are analysed and categorized into five configurations, mono-stable, multi-stable, multi-degrees-of-freedom, frequency up-conversion and stress optimization. For each configuration, working principles and compatibilities with miniaturization to MEMS scale are analysed and assessed. Additionally, several CMs are first proposed for PEHs in different configurations as inspirations and references to prompt the development of PEHs. Piezoelectric materials are also important factors in enhancing the energy harvesting performance. Characters of several widely adopted piezo-materials are summarized and compared. The metric of Normalized Power Density (NPD) is introduced to compare and assess the energy generation capability of PEHs with several widely-used piezoelectric materials and in different scales. A NPD-Volume graph is first presented based on the data collected in literature. It shows that PEHs with PZT have the highest NPD and stable energy generation performance in a wide volume range. Both the structural categorization and NPD-Volume graph provide guidance and reference for design and optimization of PEHs.

Contents

* Corresponding authors at: Tyndall National Institute, University College Cork, Cork, Ireland.
E-mail addresses: G.Hao@ucc.ie (G. Hao), zbigniew.olszewski@tyndall.ie (O.Z. Olszewski).

https://doi.org/10.1016/j.sna.2021.112743

Introduction

Powering sensors and circuit systems with energy scavenged from ambient environment is extremely promising, not only because it is eco-friendly, cost-efficient, but also this technology breaks the limitations posed by traditional batteries. It enables the distribution of electronics into inaccessible environment, such as deep wells, nuclear factories, and even human bodies, where changing or recharging batteries are challenging, risky or impossible. Benefits will also be seen in the field of IoT (Internet of Things) in particular [1], where numerous sensors are powered in a network for data exchanging wirelessly. In addition, energy harvesters themselves can be used as sensors for extreme value estimates [2]. Thanks to the advances in large scale integration technology and the improvement in low-energy-cost electronics over the past decades, the development and application of energy harvesting have been highly promoted [3,4].

In general, environmental energy exists in various forms, such as light, heat, electromagnetic fields, and mechanical vibrations. Harvesting energy from mechanical vibrations is more attractive, partially because mechanical vibrations are ubiquitous and independent of the season, weather and locations. Vibrational harvesters have relatively high energy density (about 0.3 $\mu W/mm^3$) [5,6] and the availability of low-power circuits and sensors (μW – mW range) [4] makes vibrational energy harvesting a suitable energy source for various application scenarios.

In principle, the vibrational energy harvester is analogous to an electronic power source which forces electrons to flow in electronic circuits. To realize the electromechanical coupling between mechanical and electric domains in vibrational energy harvesters, there are four main mechanisms available: piezoelectric [5,7,8], electromagnetic [9–12], electrostatic [13–15] and triboelectric [16–18]. Because of its numerous advantages, piezoelectric conversion principle has received most attention. This is because the transducers have relatively simple configurations and high conversion efficiency. Furthermore, advances in the piezoelectric MEMS and CMOS film technologies offer high–volume, wafer scale fabrication and integration capabilities. According to these advantages merits, this review focuses on piezoelectric energy harvesters (PEHs).

Resonance-based PEHs have large energy outputs because resonance significantly amplifies vibrational amplitudes and the stress generation in the piezoelectric materials. However, resonance inherently induces a high Q-factor or, in other words, a narrow bandwidth, which means a slight shift from the resonant frequency will lead to a dramatic drop of the energy output. Fig. 1(a) shows a sharp energy output line subject to frequency representing the resonance-based PEHs. For practical applications, harvesters are expected to have a wide frequency bandwidth, as illustrated in Fig. 1(b). According to the literature survey based on the *Core Collection* of *Web of Science* with topic keywords: *(energy harvest*) AND (piezoelectric) AND (vibration) AND (wide bandwidth) OR (large bandwidth) OR (broad bandwidth)*, growing attentions have been drawn over the past 10 years as reflected from the number of articles published from 2010 to 2019 as shown in Fig. 2. Although various approaches have been proposed to broaden the working bandwidth of PEHs [3,4,19–21], this problem still exists with significant worldwide research ongoing addressing many open issues.

Instead of utilizing traditional rigid joints, compliant mechanisms (CMs) transfer motion, load and energy through the deformation of flexible components [22–24], which can generate large stress/strain in deformed areas. For PEHs, stress/strain is required by piezoelectric effect to transfer vibrational energy into electric energy. It is thus practical to combine CMs with PEHs for enhancing the energy scavenging capability. In addition, other advantages of CMs, such as highly-alleviated friction, less or no assembling procedure, reduced mass, low cost, good compatibility to MEMS techniques etc. [24,25], will also benefit PEHs. In particular, the monolithic feature of CMs further enhances the scalability of PEHs from macro-scales into micro-scales. Therefore, it is necessary to carry out a comprehensive review on current PEHs from the aspect of CMs to explore potential solutions for the narrow-bandwidth problem. Such a review has not been reported.

This paper analysed and categorized current PEHs into five configurations based on their structural characteristics. The categorization is summarized in Fig. 3. Extended discussions on each configuration are detailed from Section 1 to Section 5. The compatibility of each configuration to MEMS process is also analysed and assessed. At the end of each section, several compliant structures suitable for PEHs are proposed as inspirations and references for researchers in this area. In Section 6, the energy generation capability of PEHs with several widely adopted piezoelectric materials in different scales are compared and assessed in a NPD (Normalized Power Density)-Volume graph. Conclusions and prospects are given in Section 7.

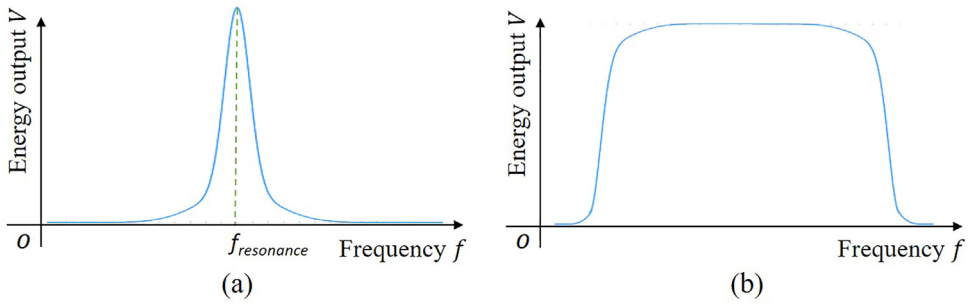

Fig. 1. Energy output- frequency graphs. (a) Resonance-based PEHs. (b) Ideal PEHs.

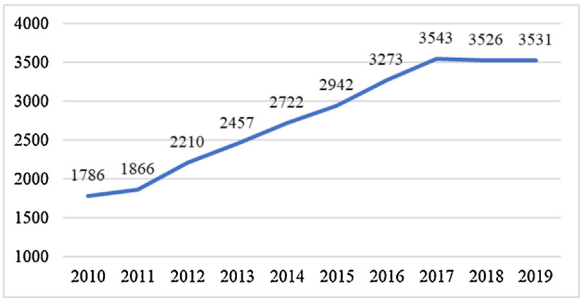

Fig. 2. The number of articles published on vibrational PEHs targeting a wide frequency bandwidth (year 2010 - 2019).

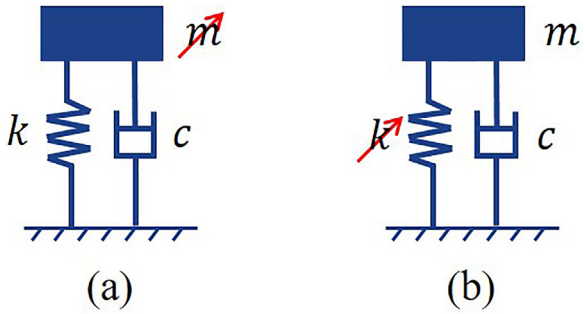

Fig. 4. Two main concepts of mono-stable PEHs for frequency tuning. (a) Modifying the mass *m*. (b) Adjusting the stiffness *k*.

1. Mono-stable structures

Mono-stable oscillators have single stable positions. Once the external stimulation stops, mono-stable oscillators eventually return to their equilibrium positions when the dynamic energy is totally damped off. PEHs in this configuration maximize the energy generation by resonance, normally in their first-order natural mode with the lowest resonant frequency and lowest stimulating energy requirement. Resonance significantly amplifies vibrational amplitudes and then the stress/strain generation for piezoelectric effect, leading to high energy outputs. Structural simplicity is another advantage of this configuration. Cantilever beams and clamped-clamped beams are two most commonly used mono-stable structures for PEHs. The mono-stable PEHs can be described through a mass-spring vibration systems and their resonant frequency, f_r, can be calculated with the equation [8,26]:

$$f_r = \frac{1}{2\pi}\sqrt{\frac{k}{m}} \tag{1}$$

Here, m represents the mass of this harvesting device, and k is the stiffness ratio.

Resonance-based devices work at the single resonant frequency [27] while environmental frequencies spread along a wide range (normally in the low frequency range below 150 Hz [4,28]). Therefore, a wide and tuneable working frequency range in a low spectrum is expected from mono-stable PEHs. According to Eq. (1), there are two ways to achieve this: (i) modifying the mass, m and (ii) adjusting the stiffness, k, as shown schematically in Fig. 4.

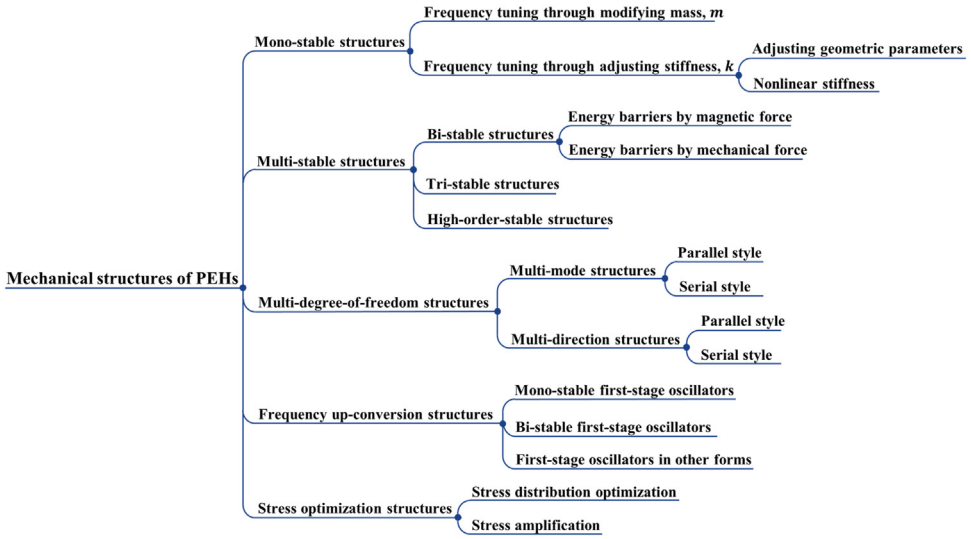

Fig. 3. Categorization of PEHs reported in literature bases on structural characteristics.

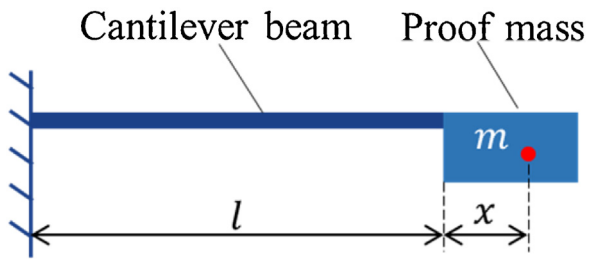

Fig. 5. Cantilever beam with tip mass.

Based on these two concepts, tuneable mono-stable PEHs for a wide frequency range can be classified into two groups.

1.1. *Frequency tuning through modifying proof mass,* m

According to Eq. (1), a larger mass leads to a lower resonant frequency when the stiffness ratio is given. Based on this principle, researchers attached proof masses on mono-stable PEHs to tune the resonant frequencies. Roundy et al. reported an energy harvester composed of a bimorph piezoelectric cantilever beam with tip-mass [29]. A power output of 375 mW was obtained at 120 Hz. Leland et al. utilized a piezoelectric bimorph attached tip-mass to power a wireless sensor for environmental monitoring [30]. The average power generated was 23.9 μW at 27 Hz. Erturk et al. presented a closed-form solution to predict the energy generation of piezoelectric cantilever beams with tip masses [31]. In experiments a maximum electric power of 23.9 mW/g^2 was obtained at 45.6 Hz. Liu et al. successfully fabricated this cantilever tip-mass structure with MEMS techniques obtaining very low operation frequency of 36 Hz [32]. Defosseux et al. also developed a cantilever tip-mass harvester in micro scale [33]. A maximum output power of 0.62 μW was observed when the excitation acceleration is 0.25 g at 214 Hz. Side effects of attaching proof mass for frequency tuning include increased total weight and decreased power density of the whole device. Targeting this issue, Berdy et al. showed a novel solution of replacing the proof mass with well-designed sensor node electronic in their mono-stable energy harvesting device [34]. A maximum power output of 198 μW was obtained at 35 Hz.

Taking the geometric position of the proof mass into consideration, as indicated in Fig. 5, the equation of the resonant frequency in Eq. (1) can be rewritten as [8,35]:

$$f_r = \frac{1}{2\pi}\sqrt{\frac{E\omega h^3}{12ml^3}\cdot\frac{r^2+6r+2}{8r^4+14r^3+\frac{21}{2}r^2+4r+\frac{2}{3}}} \tag{2}$$

E is the Yong's modulus of the material used for the cantilever, w, h, and l are the width, thickness and length of the cantilever respectively. r is the ratio between the position of tip mass gravity centre, x, and the length of the cantilever, l, which is x/l. m is the proof mass, considering the cantilever mass is negligible. According to this equation, a close distributed proof mass results in a high resonant frequency, while a far distributed mass leads to a low resonant frequency. Mass distribution in the direction perpendicular to the cantilever has no effect on the natural frequencies. Wu et al. verified this frequency tuning method both theoretically and experimentally with their prototype which was composed of a cantilever beam and a screwed tip proof mass with changeable gravity centre [36]. Through adjusting the relative position of the mass centre, a wide working frequency range (from 130 Hz to 180 Hz) was achieved. Schaufuss et al. adjusted the gravity centre through an auxiliary mass in their energy harvesting device to match the resonant frequency with driving frequency [37]. An effective working frequency bandwidth of 42 Hz–55 Hz was reported. Somkuwar et al. deployed two cylindrical masses in the tip container of a piezoelectric cantilever [38]. The equivalent gravity centre of these two masses changed when they moved to different positions and an auto-tuned resonant frequency range of 22 Hz–35 Hz was observed in experiments. Shin et al. developed an ultra-wide bandwidth PEH composed of a doubly clamped oscillating beam and a movable proof mass [39]. The resonant frequency of the device changed when the proof mass slid along the beam during device operation. This approach provided a bandwidth of 36 Hz. Shi et al. mounted a miniature stepper motor on their cantilever PEH to adjust the positon of the proof mass dynamically and an effective frequency bandwidth of 6 Hz was achieved [40]. In another approach, Jackson et al. filled the mass cavity with a liquid and used this to change the mass centre of gravity [41]. Influences of liquid density and viscosity on the performance of the nonlinearly-distributed mass were investigated.

CMs have medium degree of flexibility between rigid parts and liquids, and they provide alternative solutions for the concept of changing the centre of gravity for response broadening. During vibration of PEHs, proof masses made with compliant structures are able to change the equivalent position of gravity centre through the deformation of flexible components under the action of centrifugal force. The compliant proof mass can be fabricated in one piece with technologies like 3D printing etc. Thus, the whole device keeps monolithic. The deformation of the compliant proof mass can be pre-designed, leading to a controllable working frequency range. These unique advantages are not comparable for both rigid and liquid proof masses. One possible solution of the compliant proof mass for PEH is proposed and illustrated in Fig. 6. This compliant tip mass has 3D structures made of flexible materials, such as plastics or rubber. During oscillating, the equivalent position of gravity centre changes and this dynamically tunes the device resonance frequency and broadens its frequency response.

1.2. *Frequency tuning through adjusting stiffness,* k

In addition to the modification of proof mass, adjusting stiffness is the second way for frequency tuning of mono-stable PEHs. Stiffness is determined by several factors, including geometric parameters, loading conditions etc., and the categorization in this section is based on these factors.

1.2.1. *Stiffness adjustment with geometric parameters*

Cantilever beams with rectangular cross section are widely used for mono-stable PEHs. The stiffness ratio, k, of such cantilever beams can be calculated with the equation [8]:

$$k = \frac{3EI}{l^3} = \frac{Ewh^3}{4l^3} \tag{3}$$

Where I is the cross-section moment of inertia. According to this equation, the stiffness of the cantilever beam can be modified through changing geometric parameters (w, h and l), when the structural materials (represented with Young's modulus E in this equation) is chosen. Length, l, and thickness, h, are more influential due to their third-order power.

Jackson et al. reported a MEMS PEH with ultra-low resonant frequency (28.5 Hz) through reducing the cantilever thickness to 5 μm [42]. A peak power of 29.8 μW was observed in their experiments. One shortage of reducing the thickness is that the inevitably weakened strength of the beam and therefore also decreasing the device reliability. Increasing the length of the cantilever can lower the resonant frequency as well and to keep a compact footprint, expended cantilevers are arranged in meandering shapes. Scornec et al. achieved a tunable frequency range of 7 Hz by adjusting the effective length of the piezoelectric cantilever in their energy harvesting device [43]. Berdy et al. adopted a meandered cantilever in their PEH and a power output of 118 μW was obtained under

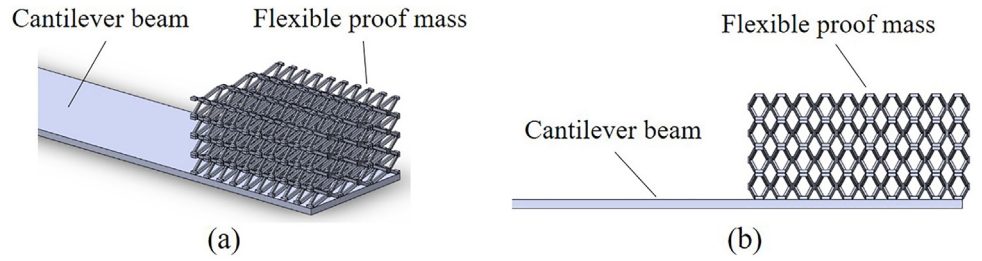

Fig. 6. Cantilever beam with deformable proof mass on tip for PEH. (a) Isometric view. (b) Side view.

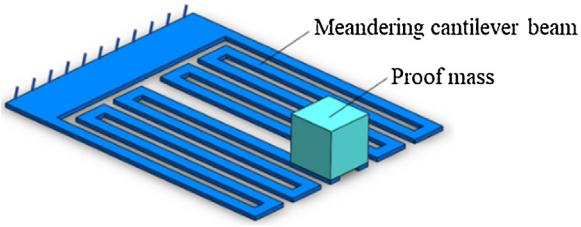

Fig. 7. Meandered cantilever beams for PEH [44].

external acceleration of 0.2 g at 49.7 Hz in experiments [44]. To eliminate the torsional stress and stress concentration, Sharpes et al. introduced a symmetric structure which contained two meandered cantilever beams in their PEH [45]. Experiments showed an energy output of 81.3 μW at 68.125 Hz with the acceleration of 0.1 g. Karami et al. investigated the possibility of powering peacemaker with a zigzag piezoelectric cantilever [46]. 10 μW power was expected to be generated under the excitation of heart beat. Liu et al. experimentally verified the low-frequency character of a S-shaped cantilever through the direct comparison with a straight counterpart for PEHs in MEMS scale [47]. To further reduce the natural frequencies of meandered cantilever beams, Apo et al. replaced straight branches with arc-based shapes [48]. Numerical models demonstrated that the frequency reduction reached up to 40 %. Wen et al. designed a MEMS PEH with a lengthened PVDF cantilever beam in a spiral shape and the working frequency of this device was about 20 Hz [49]. A MEMS-based spiral cantilever was also utilized in the PEH developed by Song et al. [50] and with an excitation of 0.25 g at 68 Hz, 23.3 nW was obtained from a five-turn spiral MEMS energy harvester. Based on the structure developed by Berdy et al., one typical meandered cantilever for PEH is shown in Fig. 7.

1.2.2. Nonlinear stiffness

When a mono-stable beam is compressed axially, its lateral stiffness is reduced. Conversely, tensile loads harden the stiffness. Frequency tuning through external loading has been adopted in PEHs and verified experimentally. Eichhorn et al. altered the resonant frequency of a cantilever beam from 380 Hz to 292 Hz by applying mechanical stress [51]. Leland et al. compressed a doubly clamped mono-stable beam axially on both sides and the resonant frequency was reduced from 250 Hz to just over 200 Hz [27]. Al-Ashtari et al. introduced tensile stress in their bimorph PEH through the attractive force between a fixed magnet and the tip magnet [52]. Experiments showed that the resonant frequency was increased by 70 %. It is noteworthy that if the mono-stable beam is compressed to buckle where the axial load exceeds the critical loading point, its original mono-stable positon collapses, and two new stable states emerge. This bi-stability of a buckled beam has caused great research interest in PEHs and will be introduced in section 2 where multi-stable devices are addressed.

During vibration, loading condition and stress distribution inside PEHs change dynamically due to the geometric deformation, which brings a nonlinear stiffness. This stiffness nonlinearity enables a broader working frequency range of mono-stable PEHs. To describe this vibrational nonlinearity, a cubic item is introduced in the differential equation of a mass-damping-stiffness oscillating system under a harmonic vibration, as presented in Eq. (4), which is also called Duffing equation [8,53].

$$m\ddot{x} + c\dot{x} + kx + \alpha x^3 = A\sin(\omega t) \tag{4}$$

x is the oscillating displacement. $A\sin(\omega t)$ is the external sinusoidal excitation and ω indicates the excitation frequency. $\dot{x}$, $\ddot{x}$ are the first and second differentiation of x with respect to time, t, which represent speed and acceleration respectively. x^3 represents the stiffness nonlinearity of the vibrating system. Constant coefficients, m, c, k, α and A, are system mass, damping rate, linear stiffness ratio, nonlinear stiffness ratio and excitation amplitude, respectively. In general, a nonlinear stiffness ratio, α, determines the nonlinearity of this oscillating system. The frequency response of displacement, x, corresponding to different nonlinear stiffness ratio, α, is shown in Fig. 8.

When the nonlinear stiffness ratio, α, is zero, Duffing Eq. (4) describes the oscillation of a linear mono-stable oscillator under sinusoidal excitation. In this case, displacement, x, reaches maximum at the resonance frequency with a narrow working bandwidth, as shown in Fig. 8(a). When α is non-zero, frequency hysteresis emerges. If α is negative, the frequency response curve bends towards lower frequency domain, which is called stiffness softening, as indicated in Fig. 8(b). Conversely, a positive α leads to stiffness hardening and the frequency response curve bends towards the higher frequency region, as illustrated in Fig. 8(c). For both stiffness softening and hardening, bended solid curves indicate a wider frequency bandwidth, but this depends on frequency sweeping directions. The internal resonance is also a nonlinear vibration phenomenon [54]. In addition to duffing nonlinear oscillations, internal-resonance-based structures have been introduced in the field of energy harvesting to broaden the frequency bandwidth [55–59]. As shown in Fig. 8(d), in this approach the response characteristic bends towards higher and lower frequency which can broaden the bandwidth regardless of the direction of the frequency sweep. Dashed lines, indicating the unstable condition that cannot be reached and will be replaced by the jump-up or jump-down behaviours between solid lines [60].

The concept of using stiffness nonlinearity in PEHs for expanding the operation bandwidth has been reported in literature and practical implementation includes three approaches: (i) geometric restriction, (ii) preloading and (iii) stoppers. In the first approach, a clamped-clamped beam is widely used whereby a beam bends and stretches during oscillation, as shown in Fig. 9. Tensional stress generated along the beam results in a hardening stiffness. Piezoelectric materials attached on deformed structures convert stress energy into electric energy by piezoelectric effect. Gafforelli et al. provided an in-depth analysis on the stiffness nonlinearity of clamped-

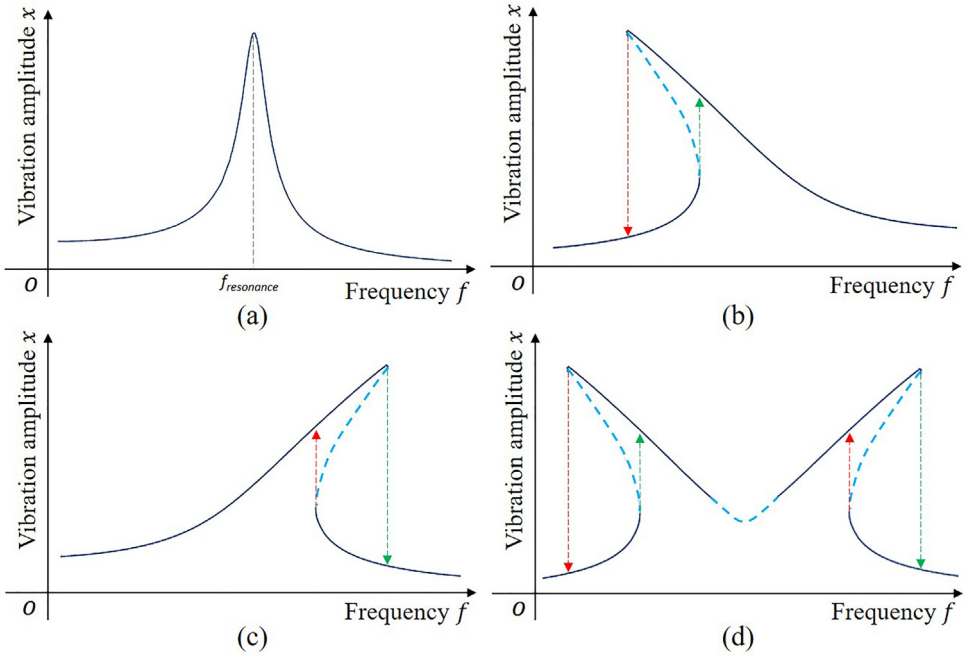

Fig. 8. Frequency response of mechanical oscillators with (a) $\alpha = 0$ (Linear stiffness); (b) $\alpha < 0$ (Nonlinear stiffness representing spring softening effect); (c) $\alpha > 0$ (Nonlinear stiffness representing spring hardening effect); (d) Internal resonance.

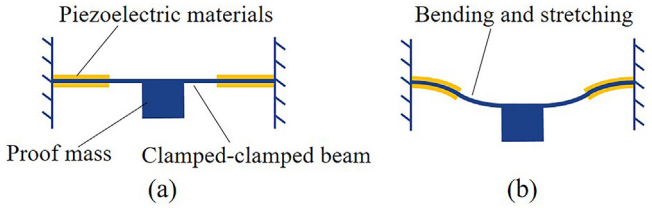

Fig. 9. Clamped-clamped beam and deformation during vibration [61]. (a) Original position. (b) Deformed beam with bending and stretching.

clamped PEHs [61]. Leadenham et al. developed a PEH based on a M-shaped doubly-clamped beam where stiffness nonlinearity was obtained under very low vibration levels (below 0.1 g and at around 5 Hz) [62]. Marzencki et al. utilized the clamped-clamped mono-stable structure in MEMS harvester [63]. Experiments verified an over 36 % adjustable frequency spectrum under 2 g excitation. Similarly, Hajati et al. developed the PEH with the doubly-clamped beam in MEMS scale [64]. A working bandwidth exceeding 20 % of the highest frequency was observed.

Preloading is the second approach to create stiffness nonlinearity. This preloading can be applied by either mechanical forces or magnetic coupling. Schematic structures of mono-stable cantilevers with different preloading conditions are illustrated in Fig. 10. The dynamically changing preloading conditions during vibration lead to the stiffness nonlinearity. To lower the working frequencies of oscillators, compression is normally adopted. Masana et al. explained the contribution of the axial preloading on the stiffness nonlinearity with an analytical model [65]. A broad working frequency range was observed in their experiments due to the stiffness hardening of a preloaded clamped-clamped beam in the pre-buckling condition [66]. Chen et al. analytically verified the wide operation frequency bandwidth introduced by stiffness hardening through compressing a clamped-clamped beam to its pre-buckling status [67]. Lin et al. applied external preloading on their piezoelectric cantilever with the nonlinear magnetic interaction between the tip magnet mounted on the cantilever and the stationary magnet fixed nearby [68]. A dynamic response over a much wider frequency range than that of a standard cantilever was obtained. Stanton et al. applied external load on the cantilever beam by the inactive force between the tip magnet and external magnets in their PEH [69]. Both stiffness softening and hardening could be achieved with the same device through adjusting the relative position of the magnets distributed. Sebald et al. expanded the working frequency range of a piezoelectric cantilever to 450 % through introducing the interaction between the tip magnet and external magnets [70]. The maximum power output was decreased by 60 % in report. Instead of a fixed external magnet, Tang et al., utilized an oscillating magnet to interact with the tip magnet of the cantilever to achieve stiffness-softening nonlinearity [71]. Verified by experiments, the working bandwidth was nearly doubled and power output was increased by 41 % compared with the counterpart with a fixed external magnet. To enhance the dynamic performance of the structure as shown in Fig. 10(b) with stiffness hardening nonlinearity, Yu et al. introduced a slider which can move freely along the cantilever [72]. Based on the interaction between the cantilever and sliding mass, the system could automatically catch the high-energy orbit increasing the power output by more than 25 times when compared to the counterpart with a fixed end mass.

For constructing of the PEHs based on the internal resonance phenomenon, a primary nonlinear oscillator is connected with a linear auxiliary oscillator as illustrated in Fig. 11(a). The nonlinear structures as shown in Fig. 10 are options for the primary oscillators. Chen et al. first proposed an energy harvester with the two-to-one internal resonance and a bi-stable oscillator was chosen as the primary oscillator in their device [55]. The wide bandwidth under a sinusoidal excitation in both frequency sweep directions was theoretically demonstrated. Although the harvester is originally based on electromagnetic mechanism, the structure proposed is transferable for PEHs. Also, Jiang et al. investigated the PEH devices based on the internal resonance, however, in their structure a buckled (preloaded) beam was used as the primary oscillator [56]. The wide bandwidth in two frequency sweep directions was also demonstrated and theoretically analysed. Xiong et al. employed the nonlinear structure as shown in Fig. 10(b) as the primary oscilla-

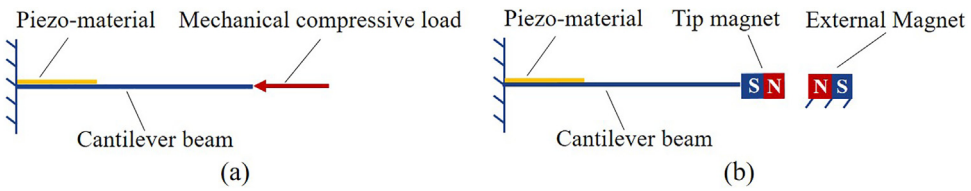

Fig. 10. Schematic structures of mono-stable piezoelectric cantilevers with (a) Mechanical pre-load [66] or (b) Magnetic coupling [68].

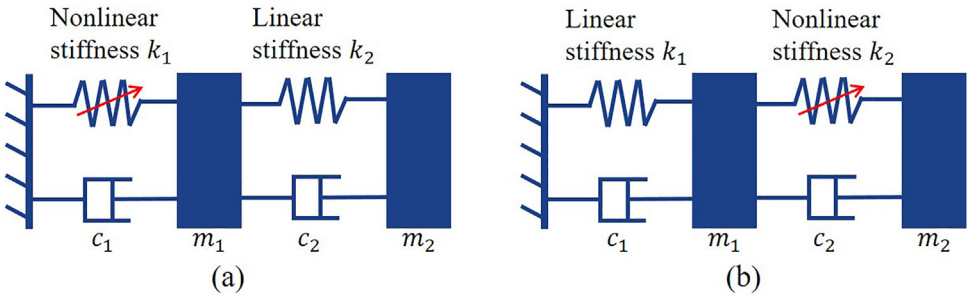

Fig. 11. Schematic structures of nonlinear oscillators based on (a) Internal resonance [55] and (b) NESs [80].

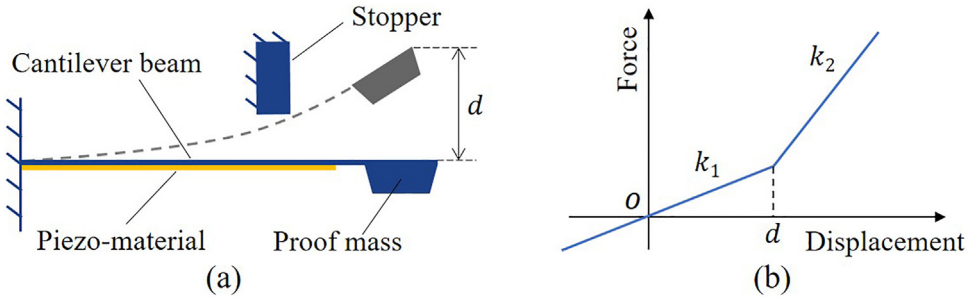

Fig. 12. A nonlinear PEH with a mechanical stopper [87] (contact aided CM [81]). (a) Schematic structure. (b) Piecewise-linear stiffness ratio.

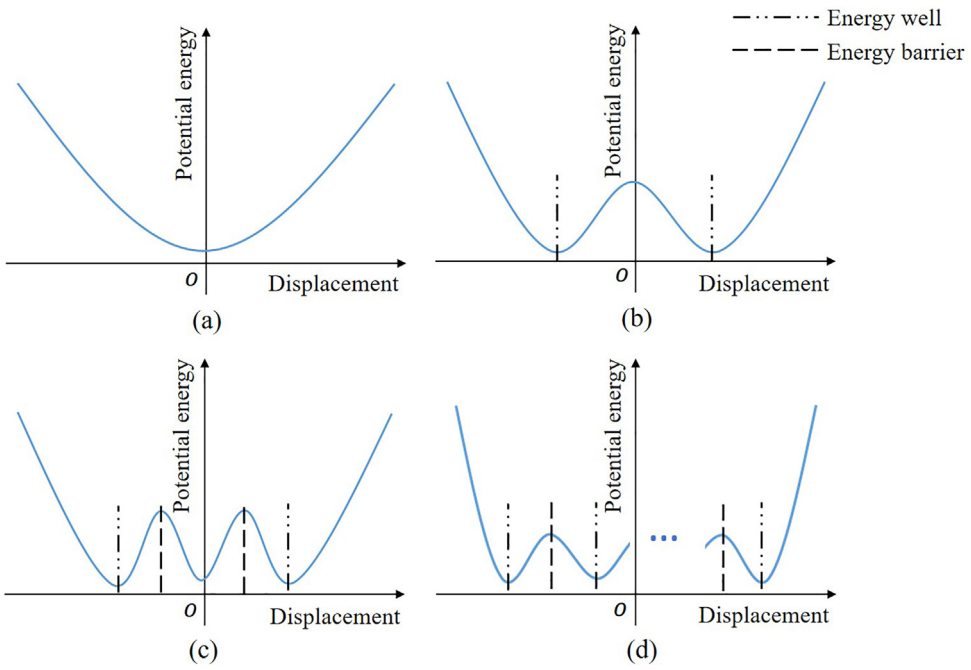

Fig. 13. Schematic potential energy graph of multi-stable structures. (a) Mono-stable type. (b) Bi-stable type. (c) Tri-stable type. (d) High-order-stable type.

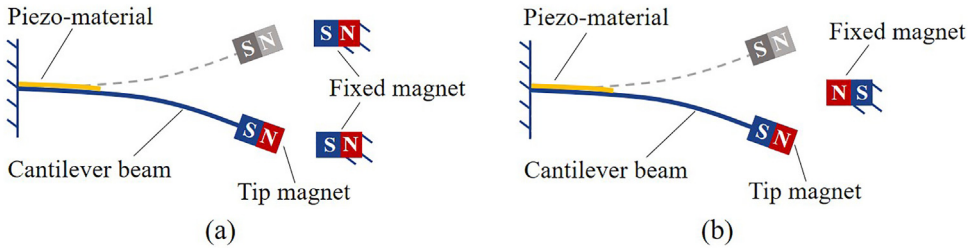

Fig. 14. Schematic structures of magnetic bi-stable energy harvesters based on (a) Attractive forces (type I) [93] and (b) Repulsive forces (type II) [94] created by fixed permanent magnet located in close proximity to the vibrating structure.

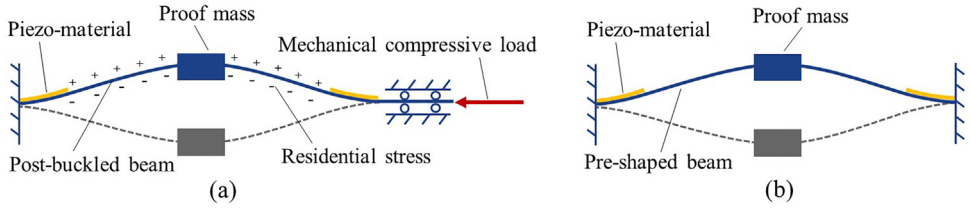

Fig. 15. Purely mechanical bi-stable structures for PEHs. (a) Post-buckling type [100]. (b) Pre-shaped type.

tor in their L-shaped PEH with the internal resonance [58,59]. A comprehensive study was carried out and the broadened frequency bandwidth was experimentally verified. Xie et al. reported a T-shaped PEH device that used a clamped-sliding nonlinear beam as the primary oscillator in connection with a linear cantilever [57]. The wide frequency bandwidth of this harvester was analytically and experimentally demonstrated. The nonlinear energy sinks (NES) responding to wide-range frequency excitation have also attracted the attentions of researchers to improve the performance of PEHs [73–79]. Different from the connecting sequence of linear and nonlinear oscillators in those internal-resonance-based structures [55–59], nonlinear oscillators (as NESs) are mounted on the linear (primary) oscillators in the NES-based structures as shown in Fig. 11(b). Under certain conditions, the vibrational energy is irreversibly pumped from the primary oscillator to the coupled nonlinear oscillators [80]. In the PEH developed by Zhang et al. [75], a NES, which consisted a prepressed clamped-clamped beam with nonlinear stiffness, was utilized to connect a primary oscillator. Experiments verified the harvester had a broadband response from the oscillation of the NES while the vibration of the primary oscillator was suppressed. In the NES-based PEH developed by Xiong et al., a piezoelectric cantilever with a magnetic tip interacting with adjacent magnets was used as the nonlinear oscillator [76]. The wide frequency bandwidth under external harmonic excitation was demonstrated. Zhang et al. proposed the application for the NES-based PEH into a special scenario in the spacecraft [77]. The PEHs based on the internal resonance and NESs can be classified into multi-degrees-of-freedom structures as summarized in section 3. They are introduced here to highlight the effect of stiffness nonlinearity in widening the frequency bandwidth.

Mono-stable PEHs coupled with stoppers also can exhibit stiffness nonlinearity. However, in this scenario the stiffness hardening happens sharply rather than gradually. A typical structure of this nonlinear PEH with a mechanical stopper and its characteristic curve of stiffness are given in Fig. 12. Once the cantilever's vibrating amplitude exceeds the distance, d, to the fixed stopper, their contact results in a shorter oscillating cantilever fixed at the contact position. The stiffness of the system is hardened from k_1 up to k_2 because of the dimension effect. Therefore, the overall system owns a piecewise-linear stiffness, as shown in Fig. 12(b). From the aspect of CMs, nonlinear-stiffness structures coupling with stoppers are also called contact aided CMs [81]. Halvorsen et al. verified the stiffness-hardening nonlinearity caused by a mechanical stopper both theoretically and experimentally [82]. A wide frequency range (110 Hz–132 Hz) was observed. Zeng et al. symmetrically arranged a mechanical stopper on each side of the piezoelectric cantilever beam for Energy harvesting [83]. A bandwidth of 7.3 Hz (51.2–58.5 Hz) was achieved. Olszewski et al. developed a PEH to scavenge energy from wires carrying AC current and the frequency bandwidth was broadened by 250 % through introducing a mechanical stopper [84]. Instead of placing stoppers on the base, Hu et al. arranged the stoppers onto a primary oscillating system in their PEH [85]. The overall device showed piecewise linear stiffness as well and a wider frequency bandwidth was obtained. To expand the effective frequency spectrum of a S-shaped piezoelectric beam in MEMS scale, Liu et al. introduced hardening stiffness through applying a mechanical stopper in their device [86]. The efficient frequency bandwidth was increased from 3.4 Hz to 11.1 Hz. The influence of stop distances and input acceleration on the frequency broadening effect were also investigated in their research. Liu et al. developed a MEMS harvester with a low resonance frequency of 36 Hz [32]. The working frequency bandwidth was widened to 17 Hz through assembling the device on a carrier with limited spacer. In spite of the advantage of widened bandwidth brought by mechanical stoppers, the energy conversion efficiency declines because of the reduced vibrating amplitude at a continuous frequency sweeping range.

1.3. Discussion

In terms of miniaturization, various mono-stable PEHs (linear or nonlinear) have been proposed due to their structural simplicity, as this has been introduced in this section. With special design, CMs exhibit stiffness nonlinearity. Howell et al. carried out a systematic research on nonlinear compliant structures [23]. Hao et al. proposed a framework for designing CMs with nonlinear stiffness and several nonlinear compliant structures based on this concept were presented [25]. Because of the inherent benefits of CMs, these nonlinear compliant structures provide references and inspirations for the design of nonlinear PEHs. In addition, mono-stable oscillators normally own the simplest structures. They can be seen as the basic elements and theoretical foundations for the construction and design of PEHs in more complex configurations in the following sections.

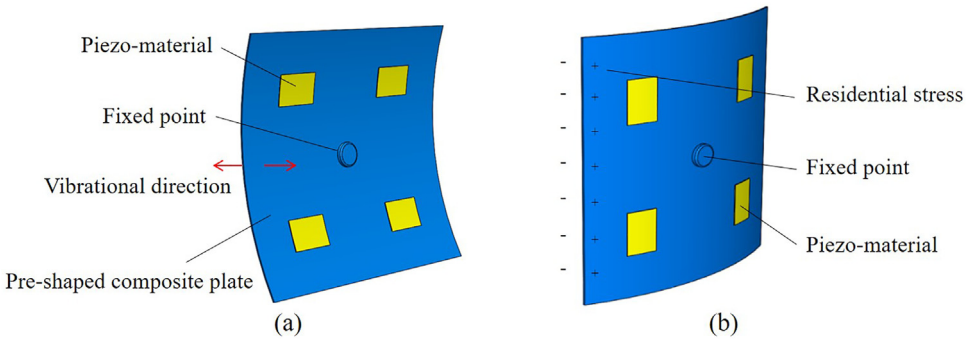

Fig. 16. Schematic structure of the bi-stable pre-shaped composite plate [110]. (a) The first/original stable position. (b) The second stable position with residential stress.

2. Multi-stable structures

Unlike devices with mono-stable configuration, which has a single stable point along the vibrating range, multi-stable structures can stay in balance in multiple positions. Each stable position represents local potential-energy minimum, and it is therefore also called the potential energy well. Between every two adjacent potential energy wells, there exists one potential energy barrier, indicating the energy required for oscillators to jump from one stable position to another. Schematic graphs of potential energy patterns along the deformation range for mono-stable and multi-stable types are given in Fig. 13. According to the number of stable positions, multi-stable configurations are subdefined as bi-stable, tri-stable, quad-stable etc. Theoretically, PEHs in multi-stable configurations have nonlinear stiffness because of the changing stiffness during oscillating. Multi-stable configurations are introduced in a separate section is to highlight their unique features for application into PEHs.

The presence of multiple stable positions brings PEHs into diverse vibrating behaviours. Depending on the excitation magnitude of environmental vibration, multi-stable oscillators vibrate in three manners, i.e. intra-well, chaotic and inter-well vibrations respectively [88]. When the environmental excitation is weak and kinetic energy provided is lower than that required to snap through energy barriers, the multi-stable oscillator can only oscillate locally around current stable positon. In this case, multi-stable oscillators show the same dynamic character as the mono-stable devices. When the environmental excitation is larger, the oscillator can jump from one stable position to another, and then an inter-well vibration is obtained. Chaotic oscillation will be triggered when the external excitation energy is between the two conditions above. In such situation, multi-stable oscillators behave in an unpredictable (chaotic) manner. To gain more energy output from PEHs, inter-well vibration is preferable because the large deformation of oscillators while snap-through behaviours lead to a higher stress generation. Therefore, multi-stable PEHs with shallower and wider energy barriers can generate more energy even under weak excitations [89,90]. Due to these advantages, the multi-stable configuration (especially bi-stable type) has drawn more attention in recent years [20,88,91,92]. Sharing the same working principles, multi-stable type devices can be seen as derivations of bi-stable oscillators.

2.1. Bi-stable structures

With designing a bi-stable oscillator the essence is to create an energy barrier between two potential energy wells. This potential energy barrier can be understood as the work of a resistance force against the vibrating motion in a certain area. Based on the nature of this impeding force, bi-stable prototypes reported can be categorized into two groups: magnetically and mechanically bi-stable structures.

2.1.1. Magnetically bi-stable structures

Magnetic forces used to create bi-stable PEHs can be either attractive or repulsive that can be achieved by different magnet alignment. Typical structures of magnetic bi-stable PEHs are given schematically in Fig. 14. A piezoelectric cantilever with a tip magnet is repelled from its original mono-stable position by attractive forces (type I) or repulsive forces (type II) from closely located fixed magnets. This results in two new stable energy positions, as described in Fig. 14(b).

Erturk et al. proposed the concept of high-energy orbits for bi-stable piezo-magneto-elastic energy harvesters (type I), as described in Fig. 14(a) [93]. It was verified experimentally that the bi-stable harvester outperformed its mono-stable counterpart in terms of generated power with the difference in the order of one magnet. To further enhance the performance of bi-stable PEHs in type-I, Zhou et al. optimized the orientation of two external magnets by introducing a small tilt [95]. To further improve the working efficiency of bi-stable magnetic PEHs, Lan et al. lowered the potential energy barrier between two potential energy wells through imposing an extra small magnet in between of two magnets in type-I structure [90]. Both experiments and theoretical analysis verified that bi-stable energy harvesters with lower energy barriers could be triggered in to an inter-well vibration more easily than those with higher barriers. In other words, a lower energy barrier makes bi-stable oscillators more sensitive to weak vibrations. A broad low-frequency operation range of 4–22 Hz was obtained. Ferrari et al. designed a bi-stable energy harvester based on structural type II [96]. Comparison experiments with respect to mono-stable cantilever counterpart showed that the voltage output was increased by 88 %. To express the oscillating nonlinearity of bi-stable PEHs in structural type II, Stanton et al. developed an analytical model which could predict key oscillating characteristics accurately [94]. Under the give excitation amplitude, the dynamic performance of bi-stable PEHs highly depends on the potential energy patterns [97]. Using the Type-II bi-stable structure schematically shown in Fig. 14(b), Yang et al. proposed a hybrid resonator with internal resonance through replacing the fixed tip magnet with a moveable magnet connected with a spring [98]. It was theoretically demonstrated that the frequency bandwidth of this hybrid device could be doubled compared with that of the bi-stable oscillator with two fixed magnets.

In terms of miniaturization, the presence of magnets makes the fabrication process complex and expensive. A MEMS harvester in bi-stable style II has been fabricated by Baglio et al. on a die (7 mm × 7 mm) [99]. Enhancement both in energy output and effective frequency bandwidth was obtained in comparison experiments with a mono-stable device under Gaussian white noise excitation. Ferrari

et al. reported a MEMS bi-stable piezo-magneto-elastic harvester in the same bi-stable type [96]. Triggered by Gaussian white noise with an upper bandwidth limit of 500 Hz, the maximum output voltage reached above 1 V in experiments.

2.1.2. Mechanically bi-stable structures

Some mechanical structures have bi-stable characters and enables bi-stable PEHs to be fabricated purely mechanically. A flexible beam buckles when it is over-compressed axially. The original single stable positon collapses and two new stable positions appear. This simple post-buckled structure provides the first approach to develop bi-stable PEHs mechanically. Bistability can also be created through pre-shaped compliant structures without any loading, which is the second method for designing mechanical bi-stable PEHs. Fig. 15 indicates these two mechanical bi-stable structures schematically. Although, a post-buckling structure and a pre-shaped structure may have similar geometric profiles, they are different from each other in fabrication, working features etc. Another difference between them is that pre-shaped bi-stable structure is stress-free in its original stable position, while the post-buckling type stores stress energy in both stable positions.

Cottone et al. created a bi-stable energy harvester in the past-buckling type [100]. Compared with the unbuckled counterpart, the enhancement in both oscillation amplitude and energy output was observed under the white noise excitation. Sneller et al. attached a proof mass in the central part of the post-buckled clamped-clamped beam to enhance its dynamic performance [101]. It was proved theoretically and experimentally that the attached central mass can both broaden the frequency range and lower the energy barrier for snap-through oscillation. With the similar doubly clamped bi-stable beam, Zhu et al. further introduced magnetic forces through the central poof mass to prompt the energy generation [102]. This magnetic force triggered the second buckling mode and made the jumping behavior between two equivalent positions easier. To reduce the influence from a fixed potential energy shape and enhance the energy generating performance of bi-stable configuration, Hosseinloo proposed an adaptive bi-stable PEH [103]. The enhanced performance was analytically verified. Andò et al. introduced a cost-efficient way to develop bi-stable energy harvesters in post-buckling style [104]. Both electrodes and piezoelectric layers were printed on a flexible PET (Poly Ethylene Terephthalate) substrate through a commercial inkjet printer. Purely mechanical bi-stable structures are more friendly to miniaturization compared with those based on magnetic force because of the absence of magnets. Andò et al. theoretically verified the advantages of a purely mechanical bi-stable structure for PEHs in MEMS scale [105]. Xu et al. fabricated a doubly clamped bi-stable energy harvester successfully in MEMS scale [106]. They utilized residential stress, rather than pre-loading, to create two stable points out of the fabrication plane. Experiments have verified a wide operating frequency range (from 50 Hz to 150 Hz) at a low acceleration of 0.2 g. For the pre-shaped bi-stable structure, it has been widely researched in the area of CMs [107–109], but the application for PEHs is rare. This is mainly because of the large positive stiffness at the initial position, which corresponds to a high resonant frequency.

Bi-stability can also be achieved through planar compliant structures in a pre-curved shape and this compliant structure has been adopted for PEHs [110]. A pre-curved composite plate stays in balance in this original shape. Under sufficient environmental excitation, it jumps to the second stable positon with an opposite curvature (as shown in Fig. 16) because of the flexibility that carbon fibre epoxy owns. This pre-curved composite plate can also be seen as a special case of the pre-shaped type (in Fig. 15(b)) in 3D. Piezoelectric patches bonded on planar surfaces convert stress energy

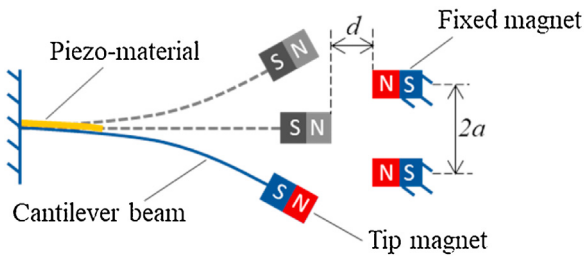

Fig. 17. Schematic structure of tri-stable piezoelectric energy harvesters utilizing repulsive force [117].

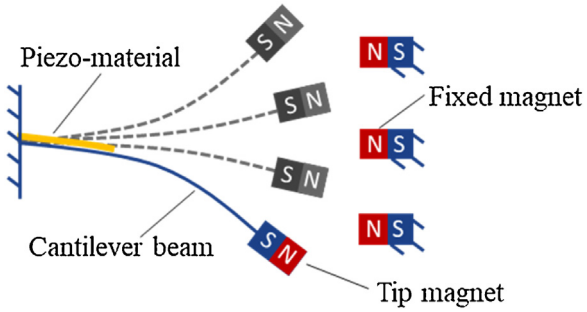

Fig. 18. Schematic structure of quad-stable piezoelectric energy harvester utilizing magnets [123].

into electric energy during the switching motion between two stable positions. Arrieta et al. and Betts et al. conducted in-depth research on the application of pre-shaped bi-stable composites for PEHs [111,112]. Both theoretical analysis and experiments verified that bi-stable composite laminates could broaden the frequency bandwidth and improve the energy output of PEHs. Arrieta et al. established a low order model to capture the dynamic response of the bi-stable composite plate [113]. The accuracy of this model was proved experimentally with a bi-stable composite plate. Instead of fixing the geometric central point, Arrieta fixed one edge of the pre-curved composite plate in a cantilevered manner in the PEH developed [114]. Bi-stability and high power conversion in a wide working bandwidth was observed in experiments.

2.2. Tri-stable structures

One more stable position is introduced along the vibrating trace of tri-stable oscillators than bi-stable oscillators. With the three equilibrium positions, more complex oscillating response to environmental vibrations is caused. Under sufficient external excitation, tri-stable oscillators jump between not only two adjacent potential wells but also two outer stable positions of the potential energy pattern (as shown in Fig. 13(c)). This larger vibrating amplitude benefits PEHs with more stress generation and higher energy output.

For PEHs with tri-stable structures, the height of the energy barriers (or the depth of the energy wells) and their distributed positions are two key factors [115]. Shallower potential energy wells increase the sensitivity of tri-stable harvesters to weak vibrations and inter-well oscillating can be triggered more easily [116,117]. A wider distance between two adjacent energy wells enlarges the deformation during inter-well vibration [118]. Due to the significant influence of potential energy barriers and wells on the dynamic performance, the design of the potential energy pattern is critical to the development of tri-stable PEHs. Theoretically, tri-stability could be created magnetically or mechanically. However, current tri-stable PEHs reported in literature were all based on magnetic forces (either attractive or repulsive). Because of

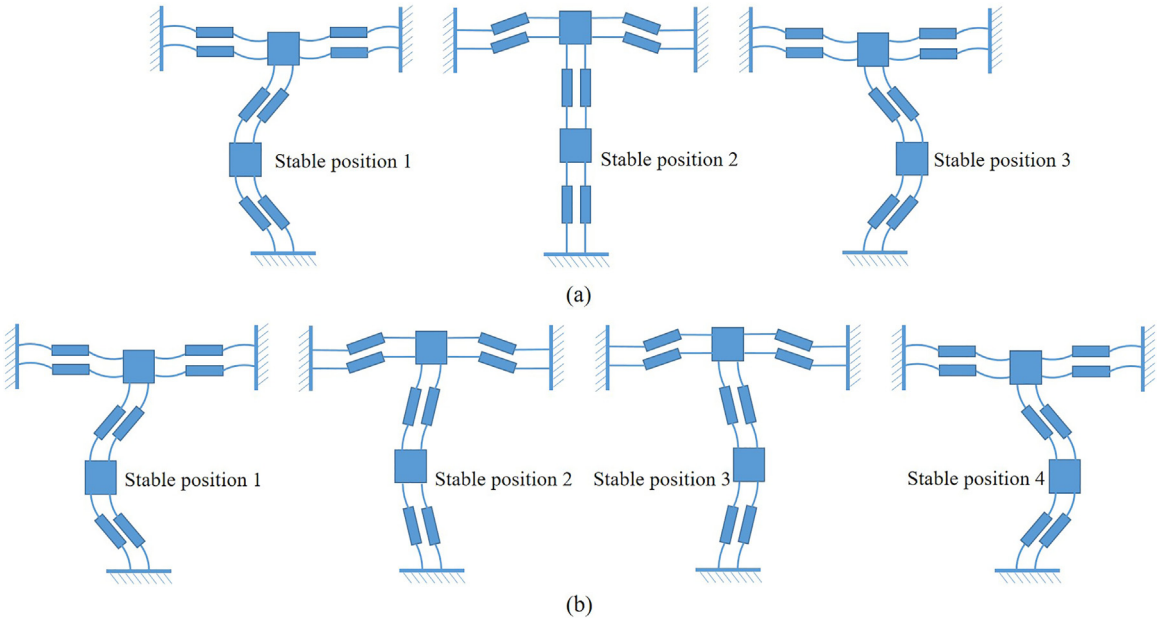

Fig. 19. Multi-stable compliant structures suitable for PEHs [128]. (a) Tri-stable compliant structure. (b) Quad-stable compliant structure.

the reduced number of external magnets utilized, repulsive force is more attractive in creating potential energy barriers for magnetic tri-stable PEHs. The schematic structure of such a magnetic tri-stable harvester is illustrated in Fig. 17.

Kim et al. [119] and Li et al. [117] investigated the influence of the geometric distribution of external magnets on the multi-stability of a cantilever-magnet device. With the same structure shown in Fig. 17, a continuous transition from mono-stable to bi-stable and then tri-stable could be achieved through adjusting the geometric parameters of d and a. The depth of potential energy wells and the relative distance between the stable positions can also be modified through changing geometric parameters, which provides a possible approach to design the potential energy patterns and dynamic behaviours of multi-stable PEHs. Zhou et al. carried out continuous and in-depth research on tri-stable piezoelectric energy harvesting [115,120]. The equivalent restoring force of the tri-stable PEHs was described as a high order polynomial for a more accurate expression of the dynamic behavior [120]. It was verified theoretically and experimentally that a wide working bandwidth at low frequency scale can be obtained under the weak vibrational excitation for tri-stale PEHs [121]. Mei et al. applied a tri-stable energy harvester to scavenge energy from rotational vibrations of a rolling vehicle wheel [122]. A wide effective rotational speed range (from 240 rpm to 440 rpm) was obtained. Utilizing the piezo-magnetic device shown in Fig. 17 with different magnetic distribution, Li et al. concluded that the tri-stable PEH showed a lower frequency threshold and higher voltage density than the bi-stable counterpart [117]. It should be noted that it is hard to compare tri-stable oscillators and bi-table oscillators without considering the depth and relative distance of the potential energy wells.

2.3. High-order-stable structures

To further enhance the advantages of multi-stable PEHs, more stable positions were created along the vibrating trace of high-order-stable configurations, such as quad-stable, Penta-stable structures. As shown in Fig. 13(d), there are n energy wells and $n-1$ energy barriers distributed along the deformation range. More complex inter-well oscillating manners will be triggered under sufficient external excitation.

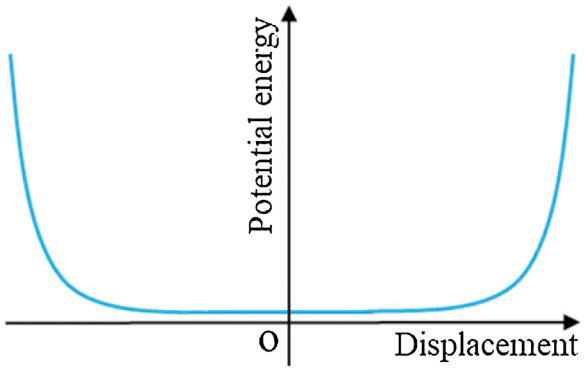

Fig. 20. Potential energy-deformation pattern of infinite-stable oscillators for PEH.

Like tri-stable embodiments introduced in section 2.2, energy barriers of high-order-stable oscillators are only created by magnetic forces (repulsive forces in particular) in report. Purely mechanical embodiments have not been seen in literature yet. The schematic structure of a piezo-magneto-elastic quad-stable harvester is illustrated in Fig. 18. Three external magnets interact with the tip magnet on the piezoelectric cantilever through repulsive forces. In this way, three potential energy barriers are created in between with every two energy wells of the four.

Zhou et al. carried out both theoretical analysis and experiments on the piezo-magnetic quad-stable energy harvesters [123,124]. Influences from external magnets distribution on the potential energy pattern of the quad-stable oscillator were investigated. In their experiments, dense snap-through vibrating behaviours among four stable positions were observed under weak excitation which brought large deformation and large energy output. Wang et al. adopted attractive magnetic force to create potential energy barriers in their magnetic quad-stable PEH [125]. The novel part was that a cantilever-surface contact was introduced to optimize the stress distribution and up-convert resonating frequencies. Experiments validated that 4.2 times more power was generated compared with its linear counterpart under a low-intensity vibration.

Based on the same magnetic principle, higher-order multi-stable PEHs were also developed. Huang et al. theoretically analysed the dynamic response of a penta-stable energy harvester to environmental vibrations [88]. It was revealed that penta-stable PEHs owned more complex oscillating behaviours, including low-energy intra-well vibrations, middle-energy inter-well vibrations and global inter-well vibration. Zhou et al. developed a penta-stable PEH in the cantilever-magnet configuration which contained a piezoelectric cantilever with tip magnet and four external magnets [126]. With shallow and largely distanced potential energy wells, frequent inter-well oscillation was observed in experiments. Kim et al. proposed a method to create penta-stability with a bimorph cantilever beam attached with a soft magnetic tip and only two external magnets [127]. The mechanism of this penta-stability was thoroughly explained and the dynamic and energetic performance of this was analysed.

2.4. Discussion

In summary, the spirit of designing a multi-stable PEHs is creating multiple equilibrium positions isolated by potential energy barriers along the vibrating trace. According to the multi-stable PEHs summarized in this chapter, magnets were widely adopted to create the multi-stability. The multi-stability and dynamic response can be easily modified through adjusting the number and geometric distribution of external magnets. However, the presence of multiple magnets makes miniaturization complex and difficult. Except bi-stable configuration, high-order multi-stable PEHs have not been either fabricated purely mechanically or in MEMS scale.

Multi-stable CMs provide multi-stability purely mechanically through the deformation of flexure segments. Their monolithic character enables the fabrication in different scales with accessible techniques, which makes multi-stable CMs a great choice for PEHs. According to authors' knowledge, PEHs based on multi-stable CMs (except bi-stable type) have not been reported yet. Howell has conducted systematic research on multi-stable CMs [23,24]. Chen et al. introduced a design principle on multi-stable CMs through the synthesis of several single bi-stable compliant structures [128–130]. Based on their research, some examples of multi-stable CMs suitable for PEHs are presented in Fig. 19. Fig. 19(a) shows a tri-stable compliant structure and a quad-stability CM is illustrated in Fig. 19(b). Integrating multiple bi-stable CMs into a sophisticated arrangement, Jin et al. [131] and Zareei et al. [132] developed multi-stable CMs with propagating motion, which could be potentially converted into PEHs in certain application scenarios.

If the number of stable positions keeps going up to extreme, such a structure will be able to stay balanced in a continuous range. Correspondingly the height of energy barriers will decline to zero and the potential energy pattern will be in a basin shape with a flat base as shown in Fig. 20. As a special case of multi-stable configuration, this can be regarded as the infinite-stable type. Statically balanced CMs (SBCMs) make such concept come true. Statically balanced behavior can be achieved through combining a positive-stiffness structure with another structure with negative stiffness. Based on this construction principle, SBCMs in various forms have been developed [133,134]. In terms of the application of this infinite-stability in PEHs, Sergio has analysed the performance theoretically [135], but further detailed research on the effective bandwidth and dynamic performance is still needed.

3. Multi-degrees-of-freedom structures

To widen the working frequency range and increase the energy output of PEHs, several mono-stable oscillators can be integrated in one single device. These mono-stable oscillating unites resonate simultaneously or individually and bring multiple degrees of freedom in the whole system level. Based on their main functions, multi-degrees-of-freedom (multi-DoF) PEHs can be sorted into two groups, multi-mode type for broadening the effective frequency bandwidth and multi-direction type aiming at scavenging vibrational energy from different directions.

3.1. Multi-mode structures

A continuous frequency range can be approximately represented by a group of isolated frequency points from this range. Based on this concept, a simple method to widen the effective frequency bandwidth of PEHs is to integrate several individual resonators with different natural frequencies to form a multi-DoF oscillator with multiple resonating modes (multi-mode). Mono-stable sub-resonators can be integrated in two methods: in parallel as an array and in series as a chain, which is shown schematically in Fig. 21. The serial type can also be seen as a single resonator with multiple resonant modes at different frequencies.

Xue et al. and Farokhi et al. numerically analysed the operating frequency bandwidth of multi-mode PEHs in array type [138,139]. It was concluded that the operating frequency bandwidth could be efficiently expanded through integrating more mono-stable resonating units. Shahruz proposed a typical multi-mode PEH with a set of piezoelectric cantilevers with different geometric parameters arranged in parallel [136]. The expanded working frequency bandwidth was verified theoretically. Feng et al. developed a micro multi-mode harvester containing four piezoelectric cantilevers in parallel [140]. In this prototype, different resonant frequencies were obtained through diversely distributed proof masses along four identical cantilever beams. A wide frequency range (from 300 Hz to 800 Hz) was achieved. Al-Ashtari et al. constructed a PEH with three piezoelectric cantilevers to broaden the efficient frequency bandwidth [141]. Dhote et al. arranged several compliant orthoplanar beams tangentially in a monolithic plane [142]. Together with the stiffness-hardening effect during vibrating, an extended frequency bandwidth of 35 Hz and a maximum peak-to-peak voltage of 4 V were obtained in experiments. For multi-mode PEHs in parallel type, the energy generation efficiency is normally low because there is only one mono-stable unit working corresponding to the excitation frequency whiles other units keep static. To improve the energy output, Zhang et al. connected every two adjacent beams with a spring to induce coupling action when either of the two resonators worked [143]. In the bi-resonant PEH proposed by Li et al., two parallel piezoelectric cantilevers coupled with each other through mechanical impact [144]. A wide frequency range of 14 Hz was obtained at the acceleration of 1 g. Deng et al. introduced magnetic interaction among parallel piezoelectric cantilevers through tip magnets [145]. A synergetic poly-stable character was observed in overall scale due to the diverse relative positions of oscillating units. In experiments the power density was increased to 760 % compared with the piezoelectric cantilever array without magnetic interaction.

Connecting mono-stable resonators in series is the second approach to construct multi-mode PEHs. Roundy et al. gave an clear explanation on this concept [137]. He proposed that a multi-mode oscillator contained n spring-mass-damper systems connected in series. The $i+1$ th sub-resonator had a resonant frequency one bandwidth away from the resonant frequency of the i th sub-resonator. A wide operating frequency range was obtained in the whole system scale. Based on this concept, Hu et al. developed a harvester containing three stages of cantilever units in a folded series way [146]. Three operating frequencies corresponding to the bending motion of three cantilever stages were obtained. Tang et al. reported a dual-mass PEH which connected two single degree of

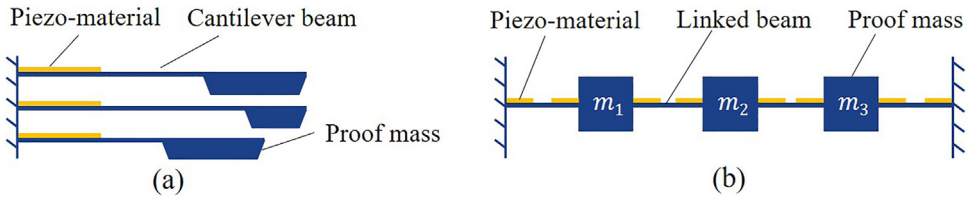

Fig. 21. Schematic structures of multi-mode PEHs. (a) Parallel style [136]. (b) Serial style [137].

freedom systems in series [147]. A better energy generation capability of this dual-mass harvester was proved with a numerical model. Tadesse et al. attached piezoelectric crystals along a slim cantilever beam to create multiple resonant modes [148]. Expanded frequency range was verified both numerically and experimentally. Gong et al. proposed a folded structure for the construction of a multi-mode harvester [149]. Energy output peaks were observed at two resonant frequencies (97 Hz and 120.9 Hz respectively) in experiments. Moon et al. proposed a method for broadening the working frequency bandwidth of a cantilever PEH through narrowing the gap between the first two resonant frequencies [150]. This was achieved through tuning parameters of the proof mass.

3.2. Multi-direction structures

In real world, environmental vibrations not only spread along a wide frequency spectrum, but also come from various directions. In practical application, it is hard to align vibration directions of energy harvesters with those of external vibrations all the time. To solve this problem and further improve the energy scavenging efficiency, PEHs sensitive to multiple vibrational directions were also investigated. Similar with multi-mode PEHs, multi-direction PEHs also integrate sub-oscillators in two ways: in parallel and in serial, as illustrated schematically in Fig. 22.

Blad et al. proposed a metric to design two-direction PEHs integrating mono-stable oscillators in series [6]. Two dimensionless parameters: the relative strength of vibrations, P_v, and the relative dimension of the design space, P_l, were identified. Based on their principle, a two-direction harvester, which vibrated in and out of the fabrication plane, was proposed. Zhou et al. developed a multi-direction harvester which consisted several piezoelectric beams linked in series and in a zigzag shape [152]. With the flexibility in two perpendicular directions, this meandering harvester was able to scavenge energy from vibrations with a wide direction range (from 0° to 90°). To harvest the vibrational energy from multiple directions, Hu et al. proposed a twisted piezoelectric cantilever beam which could be regarded as the serial style in Fig. 22(b) [153]. A substantial power output was obtained in experiment when the excitation came from any directions in the plane perpendicular to the axis of the twisted beam. Multi-direction PEHs were also developed based on the isotropic characteristics of some oscillators for vibrations from different directions. Xu et al. attached a pendulum at the tip of a piezoelectric cantilever beam which was pulled to be deformed when the pendulum was stimulated by external vibrations from multiple directions [154]. Yang et al. utilized a doubly clamped elastic rod which was sensitive to vibrations from arbitrary directions in the vertical plane in the reported multi-direction PEH [155]. When the doubly clamped elastic rod was excited to vibrate, the central piezoelectric ceramics were compressed so that the vibrational energy was converted into the electric energy. For the parallel type, Andò et al. developed a two-direction harvester composed of two piezoelectric cantilever beams perpendicular to each other [156]. In experiments, a maximum energy output of 3.2 μW was observed from each cantilever beam. Su et al. introduced magnetic repulsive forces in their tri-directional piezoelectric harvester [157]. Three mono-stable resonators were capable to scavenge energy from three mutually orthogonal directions separately. Because of the magnetic interaction, other two resonators would be triggered to resonant when one of the three oscillators was actuated by the environmental vibration. Chen et al. developed a dandelion-like PEH to capture energy from ambient vibrations in different directions, and this character was verified experimentally [151].

3.3. Discussion

Multi-mode and multi-direction configurations share the same constructing concept which is integrating mono-stable oscillators in parallel or in series. The main difference between them is that multi-mode configuration is aimed at broadening the effective frequency bandwidth, while the multi-direction configuration targets on scavenging energy from multiple directions. Due to the variety of mono-stable oscillators, distribution types, and the number of mono-table oscillators integrated, the possible form of multi-DoF PEHs shows a good diversity. Based on the sophisticated research on mono-stable PEHs (introduced in section 1), the design and fabrication of multi-mode PEHs are not difficult. In terms of miniaturization, the presence of magnets and 3D structures bring some difficulties.

A wider effective frequency bandwidth and higher energy output from multiple vibrational directions can be obtained through simply integrating more mono-stable units in one device, which is a solution for current problems of PEHs. However, some disadvantages, such as increasing volume, large weight, high cost, low power density etc. come along and a better solution is expected to be proposed.

4. Frequency up-conversion structures

Resonance significantly amplifies vibrational amplitudes of oscillators, and the energy output of PEHs at resonance is much higher than that when they are off resonance. However, the energy generation efficiency can still be low when the resonance is triggered by low-frequency vibrations because of the low-frequency deformation cycle of the piezoelectric elements. To improve the energy generation efficiency of PEHs working in such conditions, frequency up-conversion is then proposed to stimulate higher-frequency vibrations of piezoelectric elements when the environmental frequencies are low.

For frequency up-conversion PEHs, two stages of oscillators are integrated. First-stage oscillators, or driving oscillators, have low natural frequencies and they resonant with environmental vibrations. Second-stage oscillators, or generating oscillators, have higher natural frequencies and they vibrate freely when they are triggered by first-stage oscillators. Energy harvesting process is mainly completed by the second-stage piezoelectric oscillators. Interactive forces between the two stages of oscillators can be either mechanical (such as direct impact) or magnetic. Vibration character of these two stages of oscillators is shown in Fig. 23. From this aspect, frequency up-conversion devices can also be seen as fre-

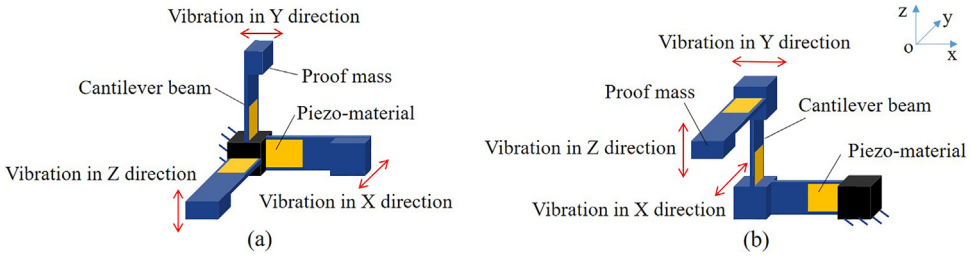

Fig. 22. Schematic structures of multi-direction PEHs. (a) Parallel style [151]. (b) Serial style [6].

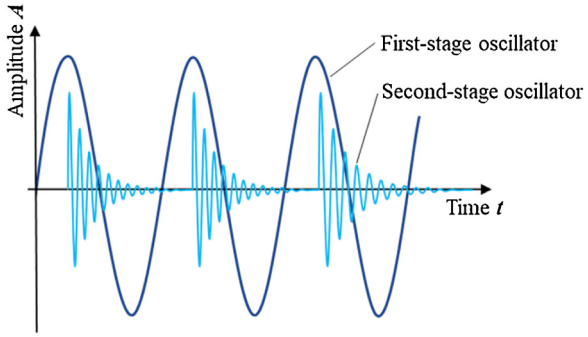

Fig. 23. Vibrational amplitudes of both stages of oscillators subject to time.

quency amplifiers. In literature, first-stage oscillators are reported in various forms, but second-stage oscillators are mainly mono-stable resonators with high resonance frequencies. In this chapter, frequency up-conversion PEHs are sorted and introduced according to their first-stage oscillators utilized.

4.1. Mono-stable first-stage oscillators

Cantilever beams are adopted as first-stage oscillators in frequency-up-conversion PEHs due to their structural simplicity. Fig. 24 schematically shows two types of interaction manners between the first-/second-stage cantilevers in such PEHs. They are mechanical impact (Fig. 24(a)) and magnetic interaction (Fig. 24(b)) respectively. Gu took a piezoelectric cantilever beam as the driving oscillator in between of two more rigid piezoelectric cantilevers as second-stage oscillators in his frequency-up-conversion harvester [158]. Through the mechanical impact, the second-stage oscillators were triggered to vibrate at their natural frequency of 280 Hz when the environmental frequency was 20.1 Hz. Compared with the first-stage piezoelectric cantilever only, the power density was increased from 13.6 $\mu W/cm^3$ to 93.2 $\mu W/cm^3$ in experiments. Ferrari et al. developed a similar frequency-up-conversion harvester based on the mechanical impact between two piezoelectric cantilever beams [159]. Experiments showed that the output voltage was roughly doubled and the efficient bandwidth was widened compared with the condition without interaction between cantilevers. Liu et al. utilized a low-frequency cantilever in the normal shape and a meandered cantilever as the first-stage oscillators separately in two MEMS frequency-up-conversion PEHs developed [47,160]. High-frequency cantilevers were chosen as second-stage oscillators. A wide operation frequency bandwidth of 14 Hz (from 12 Hz to 26 Hz) was observed in experiments. The power density reached 159.4 $\mu W/cm3$ under the acceleration of 0.8 g at 25 Hz. In addition to mechanical impact Zhang et al. introduced extra rope-driven interaction between the first-/second-stage oscillators [161]. Both simulation and experiments verified a 4 times wider working frequency bandwidth from this impact-rope hybrid device than the conventional device based on impact only. Tang et al. utilized magnetic interaction between tip magnets on the two stages of oscillators for frequency up-conversion [162,163]. The whole device had a compact footprint with all cantilevers arranged in the same plane. A peak power of 6.89 μW was scavenged from a running bus. Chen et al. adopted magnetic interaction as well for the frequency up-conversion in their harvester [164]. In Experiments, the second-stage oscillator vibrated at 85 Hz while the external excitation frequency was 40 Hz and an energy output of 0.3 mW was obtained. Magnetic interaction was also adopted by Wickenheiser et al. in the frequency-up-conversion PEH [165]. In this device the only piezoelectric cantilever beam acted as both first- and second-stage oscillators. When this cantilever vibrated with a large amplitude, closely distributed external magnets interacted with the tip magnet and caused local small-amplitude oscillation along the cantilever at a higher frequency. Galchev et al. also utilized magnetic interaction between the first-stages oscillator (a clamped-clamped PZT beam in a spiral shape) and the second-stage oscillator (a copper spring with suspended metal mass) in the frequency up-conversion harvester [166]. An average power of 3.25 μW was generated under an acceleration of 1 g at 20 Hz, and an effective frequency bandwidth of 24 Hz was created. Panthongsy et al. developed a frequency-up-conversion PEH as a floor tile to harvest the energy from human footsteps [167]. The input frequency of the upper cover was up-converted to the resonant frequency the piezoelectric cantilever through magnetic interaction.

4.2. Bi-stable first-stage oscillators

Bi-stable oscillators show better dynamic performance than mono-stable oscillators as introduced in section 2.1. Therefore, they have been also utilized as first-stage oscillators in frequency-up-conversion PEHs. Fig. 25 schematically shows two distributing manners of bi-stable structures as first-stage oscillators. Second-stage oscillators can be amounted on the base (in Fig. 25 (a)) or on the proof mass of the first-stage oscillator (in Fig. 25(b)). Andò et al. adopted a clamped-clamped bi-stable compliant beam as the first-stage oscillator and two piezoelectric cantilever beams as the second-stage oscillators in their frequency-up-conversion harvester [168,169]. In a low frequency range (0.5–7 Hz), a maximum power output of 416 μW was obtained with the acceleration of 13.35 m/s^2. Jung et al. attached second-stage piezoelectric cantilevers on the central proof mass of the first-stage bi-stable beam instead of on the frame to achieve frequency up-conversion in their PEH [170]. Second-stage oscillators were actuated to oscillate by impulsive acceleration during the snap-through buckling of the first-stage bi-stale oscillator. A maximum power output of 131 μW was obtained under the base excitation at 30 Hz. To lower the energy threshold for snap-through buckling, Han et al. fixed the first-stage bi-stable compliant beam onto two flexible sidewalls on each side [171]. Due to the outward moving tendency of the flexible sidewalls, the PEH device was sensitive to weak excitations with an acceleration of 0.5 g. Inspired by the auditory hair bundle structure,

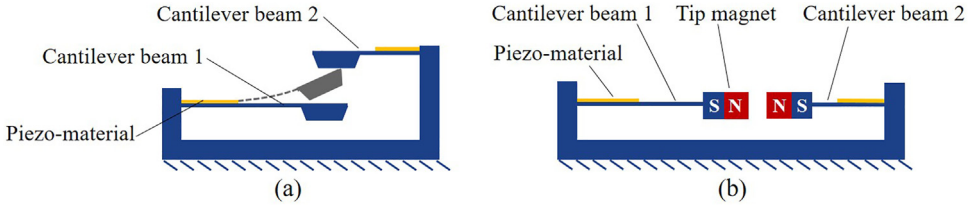

Fig. 24. Structures of frequency-up-conversion harvesters utilizing cantilvers as first-stage oscillators. (a) Coupling through mechanical impact [160]. (b) Coupling through magnetic interactions [163].

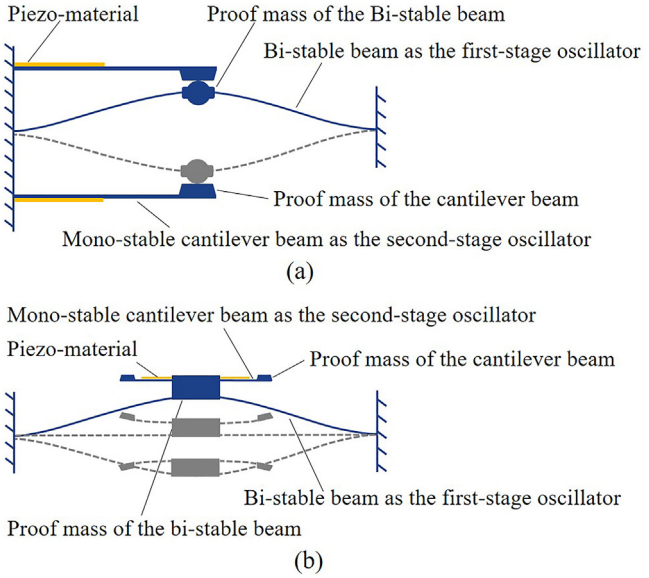

Fig. 25. Structures of frequency-up-conversion harvesters utilizing bi-stable resonators as first-stage oscillators. (a) Two stages of oscillators are distributed separately [169]. (b) Second-stage oscillators are mounted on the first-stage oscillator [170].

Kim et al. developed a bi-stable compliant mechanism as the first-stage oscillator for the frequency up-conversion harvester [172]. With this flexure structure, the free vibration of the second-stage piezoelectric oscillator at 80 Hz could be triggered by infra-low environmental vibrations at 1–10 Hz, and A maximum power output of 1.8 μW at 7 Hz was obtained in experiments. To power the peacemaker with energy from heart beats, Jackson et al. developed a shock-induced MEMS harvester which could be stimulated by the low-frequent high-acceleration heart impulses (60–240 beats per minute) and worked at its high resonant frequency of 376 Hz [173]. In this application scenario, the heart can be seen as the bi-stable first-stage oscillator while the harvester applied in heart acts as the second oscillator.

4.3. First-stage oscillators in other forms

In addition to mono-stable or bi-stable oscillators, first-stage oscillators can be in other forms. Tang et al. created a nonlinear first-stage oscillator through constraining a sliding magnet in a lubricated tube with magnetic ends [174]. Second-stage piezoelectric cantilevers were triggered by the magnetic interaction between the sliding magnet and tip magnets. An average energy output of 10 μW was obtained in the frequency range of 10 Hz–22 Hz with the acceleration of 1 g. Yeo et al. utilized an eccentric rotor (as the first-stage oscillator) to stimulate six circularly arranged PZT beams (as the second-stage oscillators) to scavenge the energy from low-frequency vibration sources [175]. A power output of 40–50 μW was produced when the device was worn on the wrist during a mild activity. Pillatsch et al. utilized a rotating pendulum as the first-stage oscillator [176]. The second-stage piezoelectric cantilever was triggered by the magnetic interaction between the magnets attached on both stages of oscillators. The energy density of 23.2 $\mu W/cm^3$ was obtained with the external acceleration of 20 m/s^2 at 2 Hz. Fan et al. adopted rolling elements (cylinder or ball) as first-stage oscillators [177,178]. The second-stage piezoelectric cantilevers were triggered by magnetic coupling forces between the tip magnets and rolling elements under external excitations. Minh et al. used a micro metal ball guided by a cylindrical hole as the first-stage oscillator in their frequency-up-conversion harvester in MEMS scale [179]. Under environmental excitation, the metal ball was stimulated to impact the piezoelectric cantilever beam arranged above. In experiments, a maximum power output of 34.6 nW was measured with the external acceleration of 39 m/s^2 in a broad working frequency range (from 20 Hz to 150 Hz).

4.4. Discussion

Frequency-up-conversion PEHs improve the energy generation efficiency through amplifying the low excitation frequencies up to higher resonant frequencies of energy-generating oscillators. Drawbacks of current frequency-up-conversion harvesters in literature include complex assembling process, large volume, difficulties in miniaturization etc. Some CMs with frequency-up-conversion character can be solutions for these problems. Tolou et al. proposed several CMs with such frequency-amplifying functions [180,181]. One of the reported structures and its working concept are illustrated in Fig. 26. Based on the elastic deformation and buckling behaviours of flexible thin beams, the monolithic mechanism can double the input frequency and export the amplified frequency at output end. Higher frequency amplification ratios are achievable through concatenating several frequency-doubling CMs in series. Benefits of such compliant frequency amplifiers include no assembling, friendliness to miniaturization, compact footprints etc. CMs also provide options for the first-stage oscillators in frequency-up-conversion PEHs. Pellegrini concluded that SBCMs were suitable for the first-stage oscillators because of their ultra-low resonant frequencies [135]. With numerical analysis, the energy generation performance was confirmed to be much better than other frequency-up-conversion PEHs in state of the art. However, only theoretical analysis was carried out and prototypes based on this concept have not been reported yet.

5. Stress optimization structures

Mechanical stress is critical for PEHs because it is basically required by the piezoelectric effect. Therefore, operations on mechanical stress, such as optimizing stress distribution and maximizing stress generation, provide new approaches to enhance the energy generation performance of PEHs. In this section, PEHs based on this concept are focused and summarized.

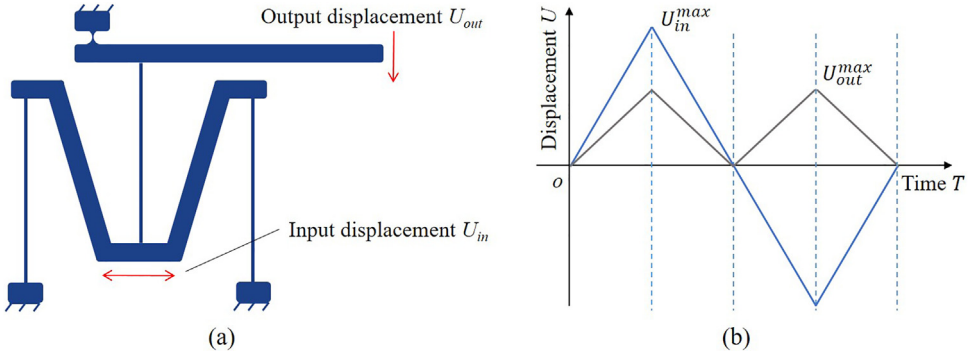

Fig. 26. Frequency doubling compliant structure proposed by Tolou et al. [181]. (a) Mechanical structure. (b) The displacement of input and output points with respect to time.

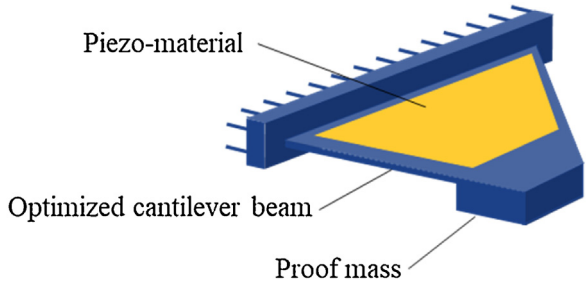

Fig. 27. Piezoelectric cantilever in trapezoidal shape for optimizing the stress distribution [182].

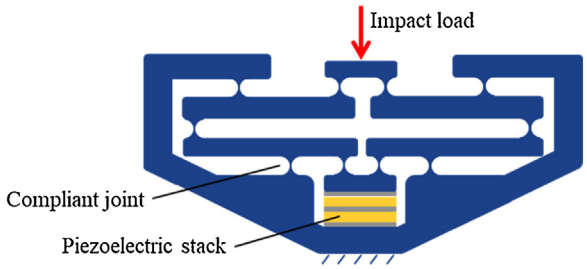

Fig. 28. Schematic structure of a compliant stress amplifier for PEH.

5.1. Stress distribution optimization

For piezoelectric cantilevers in rectangular shape, one serious problem during oscillation is the stress concentration on beams near the clamped end, while there is nearly zero stress at the free end. The unevenly distributed stress leads to a low energy conversion efficiency and short life-durance of the device. Targeting this problem, piezoelectric cantilevers with optimized shapes, such as triangular, trapezoidal etc. were proposed. The trapezoidal piezoelectric cantilever is shown schematically in Fig. 27. Roundy et al. reported that a cantilever PEH in the trapezoidal shape could double the energy output compared with that in a rectangular shape [137]. In the comparison experiments carried out by baker et al., the energy density of trapezoidal piezoelectric cantilevers was 30 % higher than that of rectangular counterparts [182]. Goldschmidtboeing et al. reported that triangular-shaped cantilever beams had larger tolerable excitation amplitude and higher power output than rectangular cantilever beams for PEHs [183]. Montazer et al. compared the energy harvesting performance of piezoelectric cantilever beams in three different geometries, i.e. near edge width quadratic, half quadratic and Trapezoidal [184]. It was verified with simulation and experiments that the near edge width quadratic shape had much higher power extraction than other two types. In MEMS scale, Jackson et al. compared the performance of PEHs with cantilever beams in trapezoidal, wide rectangular and narrow rectangular shapes through both finite-element simulation and experiments [185]. It was concluded that trapezoidal beams showed more balanced character in power density and frequency bandwidth. Minh et al. utilized a triangular piezoelectric cantilever in their MEMS frequency-up-conversion device as the second-stage oscillator to optimize the stress distribution and increase the energy output [179]. Different from shape optimization, CMs showed another solution in tackling the problem of unevenly distributed stress in the cantilever PEHs. In the prototype developed by Ma et al., a polyvinylidene diflouoride (PVDF) unimorph was fixed on the base at one end, and the other free end was attached with a complaint structure containing two flexure hinges and a proof mass for a more uniform stress distribution [186]. Compared with traditional cantilever beams in experiments, 50 % more power was produced but with a lower maximum stress under the acceleration of 0.31 g. With the same device based on the CM, Yeo et al. enhanced the energy generation performance through utilizing PZT films instead of PVDF films [187]. A power output of 149 μW was achieved under the excitation of 6 Hz with 0.1 g acceleration.

5.2. Stress amplification

In the scenario where energy is scavenged from mechanical impacts, piezoelectric stacks are used. To improve the energy generation efficiency, external impulsive force applied on piezoelectric stacks is expected to be multiplied. CMs have been adopted as such stress amplifiers in PEHs. A compliant structure with stress-amplifying function is schematically shown in Fig. 28. Based on the deformation of compliant joints and lever principle, the input load will be multiplied with a certain ratio (determined by geometric parameters) and then applied on piezoelectric stacks. Zhang et al. developed a compliant load amplifier in a pedal PEH to maximize voltage outputs [188]. The monolithic compliant structure was designed based on pseudo-rigid-body and topology theories. In experiments, a maximum power of 427 μW was generated under the load of 15 N at 1 Hz. Wen et al. designed a force-amplification CM for harvesting energy from human walking [189]. Integrating four stages of force amplifiers in a monolithic form, the device amplified the input force 17.9 times and a maximum power of 50.8 mW was observed with the input force of 65.73 N. Feenstra et al. replaced the strap buckle of a backpack with a piezoelectric stress-amplifier to scavenge energy from wearers' motions [190]. This integrated compliant structure converted and multiplied the tensile force to a larger compressive force on the piezoelectric stack. A mean energy output of about 0.4 mW was obtained in testing. For scavenging the vibration energy of pressure fluctuations in pipeline systems, Cao et al. introduced a compliant force amplifier to increase the force applied on the piezoelectric stack [191]. Such

Table 1
Comparison of piezo-materials widely used in PEHs.

Piezo-materials	Advantages	Disadvantages
PZT ($Pb[Zr_xTi_{1-x}]O_3$)	1. Excellent piezoelectric properties [192]. 2. High Curie temperatures [4].	1. Lead contained in PZT is toxic [193]. 2. Polarization process is required for piezoelectric effect [194,195].
KNN ($K_{0.5}Na_{0.5}NbO_3$)	1. Lead-free perovskites ceramics [196,197]. 2. High piezoelectric constants, good Young's modulus, moderate dielectric properties and Curie temperatures [197,198,199].	High leakage current density caused by element loss because of the thermalization problem [3].
ZnO	Good semiconducting properties; multiple forms are available [200].	1. Moderate piezoelectric properties [201]. 2. ZnO is unstable and reacts with other IC materials; 3. It is hard to reproduce its properties [202].
AlN	1. Compatible to MEMS process. Various operations can be done on it [3,202]. 2. Excellent physical properties: high thermal conductivity, high breakdown voltage, high resistivity and corrosion resistance [202,203]. 3. Biocompatible [204,205].	1. Moderate piezoelectric properties [3,201]. 2. Residual stress in AlN during fabrication has an influence on the piezoelectric performance [206].
PVDF (Polyvinylidene fluoride)	1. Outstanding flexibility, low density, good stability, tough [207]. 3. Available in the market for easy applications.	1. Poling process is required [208,209,210]. 2. Moderate piezoelectric properties [3,207].

Table 2
Energy generation capability of PEHs from literature.

Number	Power (μW)	Acceleration (g)	Volume (mm^3)	Frequency (Hz)	NPD (μW/mm3/HZ/g2)	Piezoelectric materials	Mechanical structures (corresponding sections in this review)	Source
1	118	0.2	588	49.7	1.01E-01	PZT	Mono-stable (section 1.2)	Berdy et al. 2012 [44]
2	29.3	0.05	3106	27	1.40E-01	PZT	Mono-stable (section 1.1)	Leland et al. 2004 [30]
3	23,900	1	3520	45.6	1.49E-01	PZT	Mono-stable (section 1.1)	Erturk et al. 2009 [31]
4	375	0.25	1000	120	5.00E-02	PZT	Mono-stable (section 1.1)	Roundy et al. 2004 [29]
5	0.0855	1	10.1	47	1.80E-04	PZT	Nonlinear Mono-stable (section 1.2.2)	Liu et al. 2011 [32]
6	257	1	56.4	97.6	4.67E-02	PZT	Mono-stable (section 1.1)	Shen 2009 [218]
7	2.13	2	0.652	461.15	1.77E-03	PZT	Mono-stable (section 1.1)	Shen 2009 [218]
8	0.32	0.75	0.769	183.8	4.02E-03	PZT	Mono-stable (section 1.1)	Shen 2009 [218]
9	280	0.08	50,000	26	3.37E-02	PZT	Nonlinear mono-stable (section 1.2.2)	Challa et al. 2008 [219]
10	0.0233	0.25	0.11	68	4.98E-02	PZT	Mono-stable (section 1.2.1)	Song et al. 2017 [50]
11	240	0.4	14,025	67	1.60E-03	PZT	Mono-stable (section 1.1)	Zhu et al. 2011 [220]
12	13.98	1	18.6	235	3.20E-03	PZT	Mono-stable (section 1.1)	Lei et al. 2011 [221]
13	1.11	0.39	0.99	528	1.40E-02	PZT	Mono-stable (section 1.1)	Park et al. 2010 [222]
14	43	2	1850	2	2.91E-03	PZT	Frequency up-conversion (section 4)	Pillatsch et al. 2014 [176]
15	1530	0.4	16,416[e]	20.1	2.90E-02	PZT	Frequency up-conversion (section 4)	Gu 2010 [158]
16	2.16	1	0.78	608	4.55E-03	PZT	Mono-stable (section 1.1)	Fang et al. 2006 [223]
17	2.765	2.5	0.425	255.9	4.07E-03	PZT	Mono-stable (section 1.1)	Lee et al. 2009 [224]
18	1.288	2	0.612	214	2.46E-03	PZT	Mono-stable (section 1.1)	Lee et al. 2009 [224]
19	1	1	11.9	892	9.42E-05	PZT	Mono-stable (section 1.1)	Kanno et al. 2012 [198]
20	13	1	0.153	2297	3.70E-02	PZT	Mono-stable (section 1.1)	Isarakorn et al. 2011 [225]
21	15,300	0.69	1140	29	9.72E-01	PZT	Mono-stable (section 1.1)	Cho et al. 2014 [212]
22	1.4	2	0.48	870	8.38E-04	PZT	Mono-stable (section 1.1)	Muralta et al. 2009 [226]
23	5.3	0.5	4.05	126	4.15E-02	PZT	Mono-stable (section 1.1)	Morimoto et al. 2010 [227]
24	22	4	0.021	1300	5.04E-02	PZT	Nonlinear Mono-stable (section 1.2.2)	Hajati et al. 2011 [64]
25	13.9	0.2	464	76	9.85E-03	PZT	Mono-stable (section 1.1)	Durou et al. 2010 [228]
26	0.731	1	0.306	1509	1.58E-03	KNN	Mono-stable (section 1.1)	Minh et al. 2013 [229]
27	3.62	1	2.01	132	1.36E-02	KNN	Mono-stable (section 1.1)	Won et al. 2016 [230]
28	1.1	1	11.22	1036	9.46E-05	KNN	Mono-stable (section 1.1)	Kanno et al. 2012 [198]
29	1.25	1	11.5	1300.1	8.36E-05	ZnO	Mono-stable (section 1.1)	Wang et al. 2015 [231]
30	0.00046	0.5	105.125	489.9	3.57E-08	ZnO	Multi-mode (Section 3.1)	Tao et al. 2019 [232]
31	3.5	0.2	30.7	149	1.91E-02	AlN	Mono-stable (section 1.1)	Jackson et al. 2014 [185]
32	60	2	31	572	8.46E-04	AlN	Mono-stable (section 1.1)	Elfrink et al. 2009 [233]
33	0.62	0.275	2.8	214	1.37E-02	AlN	Mono-stable (section 1.1)	Defosseux et al. 2012 [33]
34	0.18	1	1.63	853	1.29E-04	AlN	Mono-stable (section 1.1)	Hirasawa et al. 2010 [234]
35	6.9	0.2	15	599	1.92E-02	AlN	Mono-stable (section 1.1)	Elfrink et al. 2010 [235]
36	0.8	2	0.504	1495	2.65E-04	AlN	Mono-stable (section 1.1)	Marzencki et al. 2008 [236]
37	128	1	14.16	58	1.56E-01	AlN	Mono-stable (section 1.1)	Andosca et al. 2012 [237]
38	34.78	2	12.76	572	1.19E-03	AlN	Mono-stable (section 1.1)	Dow et al. 2014 [238]
39	0.669	1	2.125	315	9.99E-04	AlN	Mono-stable (section 1.1)	Jackson et al. 2013 [239]
40	18.56	1.75	280	30	7.21E-04	PVDF	Mono-stable (section 1.1)	Kim et al. 2018 [240]
41	40.9	1	41.19	164	6.05E-05	PVDF	Mono-stable (section 1.1)	Montazer et al. 2018 [184]
42	1.0688	1	267	102.9	3.89E-05	PVDF	Mono-stable (section 1.1)	Shen 2009 [218]
43	100.833	0.431	48.7	100	1.11E-01	PVDF	Mono-stable (section 1.1)	Cao et al. 2011 [241]
44	112.8	0.5	132.6	34.4	9.89E-02	PVDF	Mono-stable (section 1.1)	Song et al. 2017 [242]

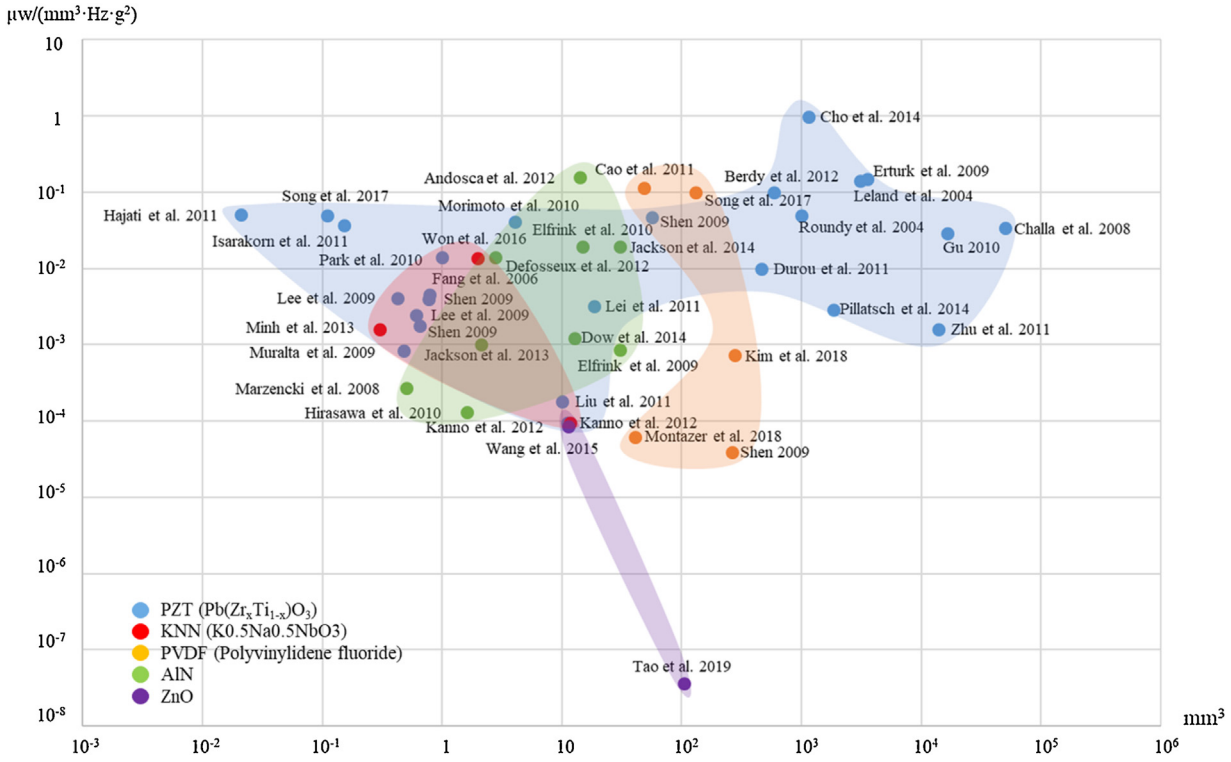

Fig. 29. NPD-Volume graph of PEHs.

stress-amplifying compliant PEHs in MEMS scale have not been reported in literature yet according to authors' knowledge.

6. Piezoelectric materials and energy generation capability of PEHs

In addition to mechanical structures, piezoelectric materials also play critical roles in PEH. Popular piezoelectric materials for PEHs include PZT ($Pb[Zr_xTi_{1-x}]O_3$), KNN ($K_{0.5}Na_{0.5}NbO_3$), ZnO, AlN and PVDF (Polyvinylidene fluoride). For a clear comparison, main characteristics of these piezo-materials are summarized in Table 1.

Due to their specific physical characters, different piezo-materials were utilized in PEHs with different structures, sizes and application scenarios. The energy generation capability varies from a device to another. To compare their energy generation performance, a normalized criterion is required. We adopt the metric of Normalized Power Density (NPD), *Power/(volume·frequency·acceleration²)*, considering the device volume, excitation frequencies and stimulating accelerations. The volume of the PEH device is an important parameter because it qualitatively reflects structural configurations (which have been introduced above), fabrication techniques used, application conditions etc. We present the NPD of different PEHs and the device volume in one graph to illustrate their relationship clearly. A large amount of data on energy generating performance of PEHs has been collected and summarized [3,44,211], however, it has not been organized in such a way. Initial data of PEHs from literature are listed in Table 2. Estimated Figures based on original publications are marked with 'e'. Volume here is the active volume of devices. Based on the data in Table 2, the NPD-Volume graph of PEHs is first shown in Fig. 29. It should be noted that inaccuracy exists in this NPD-Volume graph due to the three main reasons: 1) device volumes may be calculated in different ways by authors because no standard is established for this yet [212]. 2) The same piezo-material can be fabricated in various forms which shows different performances. For example, PZT can be in ceramics, fibres, and even flexible films which are newly developed [213,214]. 3) The number of samples is limited since not all publications on PEHs provide sufficient figures wanted. Therefore, this NPD-Volume graph of PEHs shows the NPD-Volume tendency and relationship qualitatively.

Based on this NPD-Volume graph, several conclusions can be drawn. 1) PZT owns relatively the most stable power generating capability across a wide device volume range. It also represents the largest NPD among all these piezo-materials. Because of its outstanding performance, PZT has the highest popularity. 2) AlN shows higher power density in a larger device size. 3) The NPD of KNN and ZnO has a tendency to decline when the device volume increases. 4) Around the device volume of 100 mm^3, the NPD of PVDF varies among different PEHs. In addition, according to the column of mechanical structures in Table 2, it is noteworthy that mono-stable cantilever beams are still the most popular structural type for PEHs realized. Although the NPD statistic on PEHs in this paper is not comprehensive, it can still provide reference and suggestions for material selection, structural design and optimization of PEHs.

7. Conclusion and prospects

A wide variety of solutions for PEHs has been reported in literature. However, the majority of them are still based on resonance. Although resonance significantly amplifies vibrational amplitudes and then increases power outputs of PEHs, it inherently brings a high Q-factor or, in other words, a narrow bandwidth. This means a slight shift from the resonant frequency will lead to a dramatic drop of the energy output. In addition, resonance restricts the miniaturization of PEHs because of the size effect, i.e. smaller sizes lead to higher resonating frequencies [215]. Fundamental frequencies of MEMS structures can be in the kHz level which is rare in most application environment. Ideally, PEHs are supposed to be sensitive to weak vibrations in a broad frequency range. Such devices

with satisfied performance have not been realized and solutions are expected to be explored.

Stress is basically required for piezoelectric effect. Therefore, the essence for creating ideal PEHs is to generate sufficient stress in a wide frequency spectrum. CMs transfer load, motion and energy through deformations of flexible components, and a great deal of stress is generated naturally during the working process, which fulfils the stress requirements of piezoelectric effects for energy scavenging. What's more, monolithic CMs show more beneficial aspects for PEHs, such as highly-alleviated friction, less or no assembling procedure, reduced mass, low cost, good compatibility to MEMS etc. CMs, such as SBCMs, thus show large practical value in tackling current problems in PEHs. This has been verified by the good performance of PEHs utilizing CMs.

For a better understanding of state-of-the-art solutions, this review analysed and categorized PEHs into five groups, mono-stable, multi-stable, multi degree of freedom, frequency up-conversion and stress optimization, according to their structural characteristics. In each section, the compatibility of structural configurations to MEMS process was also discussed. Some structural conceptions based on CMs principles were first proposed for different configurations as both references and inspirations for researchers in this area. Apart from mechanical structures, piezoelectric materials directly determine the energy generating capability of PEHs. The metric of NPD was introduced to compare and assess the energy generation capability of PEHs with different piezo-materials and in different scales. It is noteworthy that power limit [216,217] is another figure of merit to evaluate the energy generation efficiency of PEHs with various structures and piezoelectric materials. Based on the data collected in literature, the NPD-Volume graph on PEHs was first drawn. PEHs with PZT owned the highest NPD among all piezo-materials discussed here and stable energy generation in a large volume range. The energy generating performance of PVDF is moderate, but its mechanical flexibility is very outstanding. Both of the categorization and the NPD-Volume graph of PEHs provide guidelines and reference for the piezo-material selection, structural design and optimization of PEHs for researchers in this area. In particular, the huge application value of CMs in PEH is illustrated and highlighted in this review. With the increasing attention on the application of CMs in PEHs and the development of flexible piezoelectric materials, such as flexible PZT films [213], more PEHs bases on flexible structures with better energy generating performance are expected to be developed.

Declaration of Competing Interest

The authors declare that they have no known competing financial interests or personal relationships that could have appeared to influence the work reported in this paper.

Acknowledgements

This research is financially supported by the project of EnABLES. EnABLES (http://www.enables-project.eu/) has received funding from the EU Horizon 2020 research & innovation programme, under Grant Agreement No. 730957.

References

[1] P. Kamalinejad, et al., Wireless energy harvesting for the Internet of Things, IEEE Commun. Mag. 53 (6) (2015) 102–108.
[2] G.V. Joseph, G. Hao, V. Pakrashi, Extreme value estimates using vibration energy harvesting, J. Sound Vib. 437 (2018) 29–39.
[3] M.T. Todaro, et al., Piezoelectric MEMS vibrational energy harvesters: advances and outlook, Microelectron. Eng. 183 (2017) 23–36.
[4] H. Li, C. Tian, Z.D. Deng, Energy harvesting from low frequency applications using piezoelectric materials, Appl. Phys. Rev. 1 (4) (2014) 041301.
[5] S. Roundy, P.K. Wright, J.M. Rabaey, Energy scavenging for wireless sensor networks, in: Norwell, Springer, 2003, pp. 45–47.
[6] T. Blad, et al., Vibration energy harvesting from multi-directional motion sources, in: 2018 International Conference on Manipulation, Automation and Robotics at Small Scales (MARSS), IEEE, 2018.
[7] A. Erturk, D.J. Inman, Piezoelectric Energy Harvesting, John Wiley & Sons, 2011.
[8] T.J. Kazmierski, S. Beeby, Energy Harvesting Systems, Springer, 2014.
[9] P. Podder, et al., Magnetic tuning of nonlinear MEMS electromagnetic vibration energy harvester, J. Microelectromechanical Syst. 26 (3) (2017) 539–549.
[10] S.P. Beeby, et al., A micro electromagnetic generator for vibration energy harvesting, J. Micromech. Microeng. 17 (7) (2007) 1257.
[11] B. Yang, et al., Electromagnetic energy harvesting from vibrations of multiple frequencies, J. Micromech. Microeng. 19 (3) (2009) 035001.
[12] S. Roy, D. Mallick, K. Paul, MEMS-based vibrational energy harvesting and conversion employing micro-/nano-magnetics, IEEE Trans. Magn. 55 (7) (2019) 1–15.
[13] E.O. Torres, G.A. Rincón-Mora, Electrostatic energy-harvesting and battery-charging CMOS system prototype, IEEE Trans. Circuits Syst. I Regul. Pap. 56 (9) (2008) 1938–1948.
[14] L.G.W. Tvedt, D.S. Nguyen, E. Halvorsen, Nonlinear behavior of an electrostatic energy harvester under wide-and narrowband excitation, J. Microelectromechanical Syst. 19 (2) (2010) 305–316.
[15] P. Basset, et al., A batch-fabricated and electret-free silicon electrostatic vibration energy harvester, J. Micromech. Microeng. 19 (11) (2009) 115025.
[16] F.-R. Fan, Z.-Q. Tian, Z.L. Wang, Flexible triboelectric generator, Nano Energy 1 (2) (2012) 328–334.
[17] S. Niu, et al., Theory of sliding-mode triboelectric nanogenerators, Adv. Mater. 25 (43) (2013) 6184–6193.
[18] Z.L. Wang, Triboelectric nanogenerators as new energy technology and self-powered sensors–Principles, problems and perspectives, Faraday Discuss. 176 (2015) 447–458.
[19] S. Saadon, O. Sidek, A review of vibration-based MEMS piezoelectric energy harvesters, Energy Convers. Manage. 52 (1) (2011) 500–504.
[20] S.P. Pellegrini, et al., Bistable vibration energy harvesters: a review, J. Intell. Mater. Syst. Struct. 24 (11) (2013) 1303–1312.
[21] H. Liu, et al., A comprehensive review on piezoelectric energy harvesting technology: materials, mechanisms, and applications, Appl. Phys. Rev. 5 (4) (2018) 041306.
[22] N. Lobontiu, Compliant Mechanisms: Design of Flexure Hinges, CRC press, 2002.
[23] L.L. Howell, Compliant Mechanisms, John Wiley & Sons, 2001.
[24] L.L. Howell, et al., Handbook of Compliant Mechanisms, Wiley Online Library, 2013.
[25] G. Hao, A framework of designing compliant mechanisms with nonlinear stiffness characteristics, Microsyst. Technol. 24 (4) (2018) 1795–1802.
[26] S.S. Rao, Vibration of Continuous Systems, Vol. 464, Wiley Online Library, 2007.
[27] E.S. Leland, P.K. Wright, Resonance tuning of piezoelectric vibration energy scavenging generators using compressive axial preload, Smart Mater. Struct. 15 (5) (2006) 1413.
[28] S.-G. Kim, S. Priya, I. Kanno, Piezoelectric MEMS for energy harvesting, MRS Bull. 37 (11) (2012) 1039–1050.
[29] S. Roundy, P.K. Wright, A piezoelectric vibration based generator for wireless electronics, Smart Mater. Struct. 13 (5) (2004) 1131.
[30] E.S. Leland, E.M. Lai, P.K. Wright, A self-powered wireless sensor for indoor environmental monitoring, in: Wireless Networking Symposium, University of Texas at Austin Department of Electrical & Computer Engineering, 2004.
[31] A. Erturk, D.J. Inman, An experimentally validated bimorph cantilever model for piezoelectric energy harvesting from base excitations, Smart Mater. Struct. 18 (2) (2009) 025009.
[32] H. Liu, et al., Piezoelectric MEMS energy harvester for low-frequency vibrations with wideband operation range and steadily increased output power, J. Microelectromechanical Syst. 20 (5) (2011) 1131–1142.
[33] M. Defosseux, et al., Highly efficient piezoelectric micro harvester for low level of acceleration fabricated with a CMOS compatible process, Sens. Actuators A Phys. 188 (2012) 489–494.
[34] D.F. Berdy, et al., Wide-bandwidth, meandering vibration energy harvester with distributed circuit board inertial mass, Sens. Actuators A Phys. 188 (2012) 148–157.
[35] W. Thomson, Theory of Vibration With Applications, CrC Press, 2018.
[36] X. Wu, et al., A Frequency Adjustable Vibration Energy Harvester, Proceedings of PowerMEMS, 2008, pp. 245–248.
[37] J. Schaufuss, D. Scheibner, J. Mehner, New approach of frequency tuning for kinetic energy harvesters, Sens. Actuators A Phys. 171 (2) (2011) 352–360.
[38] R. Somkuwar, J. Chandwani, R. Deshmukh, Wideband auto-tunable vibration energy harvester using change in centre of gravity, Microsyst. Technol. 24 (7) (2018) 3033–3044.
[39] Y.-H. Shin, et al., Automatic resonance tuning mechanism for ultra-wide bandwidth mechanical energy harvesting, Nano Energy 77 (2020) 104986.
[40] G. Shi, et al., A broadband piezoelectric energy harvester with movable mass for frequency active self-tuning, Smart Mater. Struct. 29 (5) (2020) 055023.

[41] N. Jackson, et al., Widening the bandwidth of vibration energy harvesters using a liquid-based non-uniform load distribution, Sens. Actuators A Phys. 246 (2016) 170–179.
[42] N. Jackson, et al., Ultralow-frequency PiezoMEMS energy harvester using thin-film silicon and parylene substrates, J. Micro/nanolithography Mems Moems 17 (1) (2018) 015005.
[43] J. Le Scornec, et al., Frequency tunable, flexible and low cost piezoelectric micro-generator for energy harvesting, Sens. Actuators A Phys. (2020) 112148.
[44] D.F. Berdy, et al., Low-frequency meandering piezoelectric vibration energy harvester, IEEE Trans. Ultrason. Ferroelectr. Freq. Control 59 (5) (2012) 846–858.
[45] N. Sharpes, A. Abdelkefi, S. Priya, Two-dimensional concentrated-stress low-frequency piezoelectric vibration energy harvesters, Appl. Phys. Lett. 107 (9) (2015) 093901.
[46] M. Amin Karami, D.J. Inman, Powering pacemakers from heartbeat vibrations using linear and nonlinear energy harvesters, Appl. Phys. Lett. 100 (4) (2012) 042901.
[47] H. Liu, et al., Piezoelectric MEMS-based wideband energy harvesting systems using a frequency-up-conversion cantilever stopper, Sens. Actuators A Phys. 186 (2012) 242–248.
[48] D.J. Apo, M. Sanghadasa, S. Priya, Vibration modeling of arc-based cantilevers for energy harvesting applications, Energy Harvest. Syst. 1 (1–2) (2014) 57–68.
[49] W. Liu, et al., Low frequency wide bandwidth MEMS energy harvester based on spiral-shaped PVDF cantilever, Sci. China Ser. E Technol. Sci. 57 (6) (2014) 1068–1072.
[50] H.-C. Song, et al., Ultra-low resonant piezoelectric MEMS energy harvester with high power density, J. Microelectromechanical Syst. 26 (6) (2017) 1226–1234.
[51] C. Eichhorn, F. Goldschmidtboeing, P. Woias, A Frequency Tunable Piezoelectric Energy Converter Based on a Cantilever Beam, Proceedings of PowerMEMS 9 (12) (2008) 309–312.
[52] W. Al-Ashtari, et al., Frequency tuning of piezoelectric energy harvesters by magnetic force, Smart Mater. Struct. 21 (3) (2012) 035019.
[53] I. Kovacic, M.J. Brennan, The Duffing Equation: Nonlinear Oscillators and Their Behaviour, John Wiley & Sons, 2011.
[54] A.H. Nayfeh, Nonlinear Interactions: Analytical, Computational and Experimental Methods, Wiley, 2000.
[55] L.-Q. Chen, W.-A. Jiang, Internal resonance energy harvesting, J. Appl. Mech. 82 (3) (2015).
[56] W.-A. Jiang, L.-Q. Chen, H. Ding, Internal resonance in axially loaded beam energy harvesters with an oscillator to enhance the bandwidth, Nonlinear Dyn. 85 (4) (2016) 2507–2520.
[57] Z. Xie, et al., Design, analysis and experimental study of a T-shaped piezoelectric energy harvester with internal resonance, Smart Mater. Struct. 28 (8) (2019) 085027.
[58] L. Xiong, L. Tang, B.R. Mace, Internal resonance with commensurability induced by an auxiliary oscillator for broadband energy harvesting, Appl. Phys. Lett. 108 (20) (2016) 203901.
[59] L. Xiong, L. Tang, B.R. Mace, A comprehensive study of 2: 1 internal-resonance-based piezoelectric vibration energy harvesting, Nonlinear Dyn. 91 (3) (2018) 1817–1834.
[60] M. Brennan, et al., On the jump-up and jump-down frequencies of the Duffing oscillator, J. Sound Vib. 318 (4–5) (2008) 1250–1261.
[61] G. Gafforelli, et al., Modeling of a bridge-shaped nonlinear piezoelectric energy harvester, Energy Harvest. Syst. 1 (3–4) (2014) 179–187.
[62] S. Leadenham, A. Erturk, Nonlinear M-shaped broadband piezoelectric energy harvester for very low base accelerations: primary and secondary resonances, Smart Mater. Struct. 24 (5) (2015) 055021.
[63] M. Marzencki, M. Defosseux, S. Basrour, MEMS vibration energy harvesting devices with passive resonance frequency adaptation capability, J. Microelectromechanical Syst. 18 (6) (2009) 1444–1453.
[64] A. Hajati, S.-G. Kim, Ultra-wide bandwidth piezoelectric energy harvesting, Appl. Phys. Lett. 99 (8) (2011) 083105.
[65] R. Masana, M.F. Daqaq, Electromechanical modeling and nonlinear analysis of axially loaded energy harvesters, J. Vib. Acoust. 133 (1) (2011).
[66] R. Masana, M.F. Daqaq, Response of duffing-type harvesters to band-limited noise, J. Sound Vib. 332 (25) (2013) 6755–6767.
[67] Y. Chen, Z. Yan, Nonlinear analysis of axially loaded piezoelectric energy harvesters with flexoelectricity, Int. J. Mech. Sci. 173 (2020) 105473.
[68] J.-T. Lin, B. Lee, B. Alphenaar, The magnetic coupling of a piezoelectric cantilever for enhanced energy harvesting efficiency, Smart Mater. Struct. 19 (4) (2010) 045012.
[69] S.C. Stanton, C.C. McGehee, B.P. Mann, Reversible hysteresis for broadband magnetopiezoelastic energy harvesting, Appl. Phys. Lett. 95 (17) (2009) 174103.
[70] G. Sebald, et al., Experimental Duffing oscillator for broadband piezoelectric energy harvesting, Smart Mater. Struct. 20 (10) (2011) 102001.
[71] L. Tang, Y. Yang, A nonlinear piezoelectric energy harvester with magnetic oscillator, Appl. Phys. Lett. 101 (9) (2012) 094102.
[72] L. Yu, L. Tang, T. Yang, Piezoelectric passive self-tuning energy harvester based on a beam-slider structure, J. Sound Vib. 489 (2020) 115689.
[73] A. Vakakis, Inducing passive nonlinear energy sinks in vibrating systems, J. Vib. Acoust. 123 (3) (2001) 324–332.
[74] X. Jiang, et al., Steady state passive nonlinear energy pumping in coupled oscillators: theoretical and experimental results, Nonlinear Dyn. 33 (1) (2003) 87–102.
[75] Y. Zhang, L. Tang, K. Liu, Piezoelectric energy harvesting with a nonlinear energy sink, J. Intell. Mater. Syst. Struct. 28 (3) (2017) 307–322.
[76] L. Xiong, et al., Broadband piezoelectric vibration energy harvesting using a nonlinear energy sink, J. Phys. D Appl. Phys. 51 (18) (2018) 185502.
[77] Y. Zhang, Y. Lu, L. Chen, Energy harvesting via nonlinear energy sink for whole-spacecraft, Sci. China Ser. E Technol. Sci. 62 (9) (2019) 1483–1491.
[78] L. Xiong, et al., Effect of electromechanical coupling on dynamic characteristics of a piezoelectric nonlinear energy sink system, Journal of Vibration Engineering & Technologies (2020) 1–13.
[79] X. Li, et al., Dynamics and evaluation of a nonlinear energy sink integrated by a piezoelectric energy harvester under a harmonic excitation, J. Vib. Control. 25 (4) (2019) 851–867.
[80] H. Ding, L.-Q. Chen, Designs, analysis, and applications of nonlinear energy sinks, Nonlinear Dyn. 100 (2020) 3061–3107.
[81] N.D. Mankame, G. Ananthasuresh, Topology optimization for synthesis of contact-aided compliant mechanisms using regularized contact modeling, Comput. Struct. 82 (15–16) (2004) 1267–1290.
[82] L.-C.J. Blystad, E. Halvorsen, A piezoelectric energy harvester with a mechanical end stop on one side, Microsyst. Technol. 17 (4) (2011) 505–511.
[83] Z. Zeng, et al., Excellent performances of energy harvester using cantilever driving double-clamped 0.7 Pb (Mg1/3Nb2/3) O3-0.3 PbTiO3 plates and symmetric middle-stops, Appl. Phys. Lett. 107 (17) (2015) 173502.
[84] O.Z. Olszewski, et al., Evaluation of vibrational PiezoMEMS harvester that scavenges energy from a magnetic field surrounding an AC current-carrying wire, J. Microelectromechanical Syst. 26 (6) (2017) 1298–1305.
[85] G. Hu, et al., A two-degree-of-freedom piezoelectric energy harvester with stoppers for achieving enhanced performance, Int. J. Mech. Sci. 149 (2018) 500–507.
[86] H. Liu, et al., A new S-shaped MEMS PZT cantilever for energy harvesting from low frequency vibrations below 30 Hz, Microsyst. Technol. 18 (4) (2012) 497–506.
[87] M. Soliman, et al., A wideband vibration-based energy harvester, J. Micromech. Microeng. 18 (11) (2008) 115021.
[88] D. Huang, S. Zhou, G. Litak, Theoretical analysis of multi-stable energy harvesters with high-order stiffness terms, Commun. Nonlinear Sci. Numer. Simul. 69 (2019) 270–286.
[89] B. Ando, How can energy be scavenged from wideband vibrations? IEEE Instrum. Meas. Mag. 18 (1) (2015) 40–44.
[90] C. Lan, W. Qin, Enhancing ability of harvesting energy from random vibration by decreasing the potential barrier of bistable harvester, Mech. Syst. Signal Process. 85 (2017) 71–81.
[91] R.L. Harne, K. Wang, A review of the recent research on vibration energy harvesting via bistable systems, Smart Mater. Struct. 22 (2) (2013) 023001.
[92] S. Baglio, et al., Energy harvesting from weak random vibrations: Bistable strategies and architectures for MEMS devices., in: 2012 IEEE 55th International Midwest Symposium on Circuits and Systems (MWSCAS), IEEE, 2012.
[93] A. Erturk, D.J. Inman, Broadband piezoelectric power generation on high-energy orbits of the bistable Duffing oscillator with electromechanical coupling, J. Sound Vib. 330 (10) (2011) 2339–2353.
[94] S.C. Stanton, C.C. McGehee, B.P. Mann, Nonlinear dynamics for broadband energy harvesting: investigation of a bistable piezoelectric inertial generator, Physica D 239 (10) (2010) 640–653.
[95] S. Zhou, et al., Enhanced broadband piezoelectric energy harvesting using rotatable magnets, Appl. Phys. Lett. 102 (17) (2013) 173901.
[96] M. Ferrari, et al., Improved energy harvesting from wideband vibrations by nonlinear piezoelectric converters, Sens. Actuators A Phys. 162 (2) (2010) 425–431.
[97] R. Masana, M.F. Daqaq, Relative performance of a vibratory energy harvester in mono-and bi-stable potentials, J. Sound Vib. 330 (24) (2011) 6036–6052.
[98] W. Yang, S. Towfighian, A hybrid nonlinear vibration energy harvester, Mech. Syst. Signal Process. 90 (2017) 317–333.
[99] B. Ando, et al., Nonlinear mechanism in MEMS devices for energy harvesting applications, J. Micromech. Microeng. 20 (12) (2010) 125020.
[100] F. Cottone, et al., Piezoelectric buckled beams for random vibration energy harvesting, Smart Mater. Struct. 21 (3) (2012) 035021.
[101] A. Sneller, P. Cette, B. Mann, Experimental investigation of a post-buckled piezoelectric beam with an attached central mass used to harvest energy. Proceedings of the Institution of Mechanical Engineers, Part I: Journal of Systems and Control Engineering 225 (4) (2011) 497–509.
[102] Y. Zhu, J.W. Zu, Enhanced buckled-beam piezoelectric energy harvesting using midpoint magnetic force, Appl. Phys. Lett. 103 (4) (2013) 041905.
[103] A. Haji Hosseinloo, Nonlinear Vibration Energy Harvesting: Fundamental Limits, Robustness Issues, and Practical Approaches, Massachusetts Institute of Technology., 2018.
[104] B. Andò, et al., A nonlinear energy harvester by direct printing technology, Procedia Eng. 47 (2012) 933–936.
[105] B. Ando, et al., Investigation on mechanically bistable MEMS devices for energy harvesting from vibrations, J. Microelectromechanical Syst. 21 (4) (2012) 779–790.
[106] R. Xu, S. Kim, Low-frequency, low-G MEMS Piezoelectric Energy Harvester. In Journal of Physics: Conference Series, IOP Publishing, 2015.

[107] G. Hao, J. Mullins, On the comprehensive static characteristic analysis of a translational bistable mechanism, Proc. Inst. Mech. Eng. Part C J. Mech. Eng. Sci. 230 (20) (2016) 3803–3817.
[108] G. Chen, F. Ma, Kinetostatic modeling of fully compliant bistable mechanisms using Timoshenko beam constraint model, J. Mech. Des. 137 (2) (2015).
[109] J. Qiu, J.H. Lang, A.H. Slocum, A curved-beam bistable mechanism, J. Microelectromechanical Syst. 13 (2) (2004) 137–146.
[110] S.A. Emam, D.J. Inman, A review on bistable composite laminates for morphing and energy harvesting, Appl. Mech. Rev. 67 (6) (2015) 060803.
[111] D.N. Betts, et al., Optimal configurations of bistable piezo-composites for energy harvesting, Appl. Phys. Lett. 100 (11) (2012) 114104.
[112] A. Arrieta, et al., A piezoelectric bistable plate for nonlinear broadband energy harvesting, Appl. Phys. Lett. 97 (10) (2010) 104102.
[113] A. Arrieta, S. Neild, D. Wagg, Nonlinear dynamic response and modeling of a bi-stable composite plate for applications to adaptive structures, Nonlinear Dyn. 58 (1–2) (2009) 259.
[114] A. Arrieta, et al., Broadband vibration energy harvesting based on cantilevered piezoelectric bi-stable composites, Appl. Phys. Lett. 102 (17) (2013) 173904.
[115] S. Zhou, L. Zuo, Nonlinear dynamic analysis of asymmetric tristable energy harvesters for enhanced energy harvesting, Commun. Nonlinear Sci. Numer. Simul. 61 (2018) 271–284.
[116] J. Cao, et al., Influence of potential well depth on nonlinear tristable energy harvesting, Appl. Phys. Lett. 106 (17) (2015) 173903.
[117] L. Haitao, et al., Dynamics and coherence resonance of tri-stable energy harvesting system, Smart Mater. Struct. 25 (1) (2015) 015001.
[118] S. Zhou, et al., Harmonic balance analysis of nonlinear tristable energy harvesters for performance enhancement, J. Sound Vib. 373 (2016) 223–235.
[119] P. Kim, J. Seok, Dynamic and energetic characteristics of a tri-stable magnetopiezoelastic energy harvester, Mech. Mach. Theory 94 (2015) 41–63.
[120] S. Zhou, et al., Broadband tristable energy harvester: modeling and experiment verification, Appl. Energy 133 (2014) 33–39.
[121] S. Zhou, et al., Exploitation of a tristable nonlinear oscillator for improving broadband vibration energy harvesting, The European Physical Journal-Applied Physics 67 (3) (2014).
[122] X. Mei, et al., A tri-stable energy harvester in rotational motion: modeling, theoretical analyses and experiments, J. Sound Vib. (2019) 115142.
[123] Z. Zhou, W. Qin, P. Zhu, Improve efficiency of harvesting random energy by snap-through in a quad-stable harvester, Sens. Actuators A Phys. 243 (2016) 151–158.
[124] Z. Zhou, W. Qin, P. Zhu, Harvesting performance of quad-stable piezoelectric energy harvester: modeling and experiment, Mech. Syst. Signal Process. 110 (2018) 260–272.
[125] C. Wang, et al., A low-frequency, wideband quad-stable energy harvester using combined nonlinearity and frequency up-conversion by cantilever-surface contact, Mech. Syst. Signal Process. 112 (2018) 305–318.
[126] Z. Zhou, et al., Improving efficiency of energy harvesting by a novel penta-stable configuration, Sens. Actuators A Phys. 265 (2017) 297–305.
[127] P. Kim, J. Seok, A multi-stable energy harvester: dynamic modeling and bifurcation analysis, J. Sound Vib. 333 (21) (2014) 5525–5547.
[128] G. Chen, Y. Gou, A. Zhang, Synthesis of compliant multistable mechanisms through use of a single bistable mechanism, J. Mech. Des. 133 (8) (2011) 081007.
[129] G. Chen, F. Ma, Kinetostatic modeling of fully compliant bistable mechanisms using Timoshenko beam constraint model, J. Mech. Des. 137 (2) (2015) 022301.
[130] G. Chen, Q. Han, K. Jin, A fully compliant tristable mechanism employing both tensural and compresural segments, J. Mech. Robot. 12 (1) (2020).
[131] L. Jin, et al., Guided transition waves in multistable mechanical metamaterials, Proc. Natl. Acad. Sci. 117 (5) (2020) 2319–2325.
[132] A. Zareei, B. Deng, K. Bertoldi, Harnessing transition waves to realize deployable structures, Proc. Natl. Acad. Sci. 117 (8) (2020) 4015–4020.
[133] N. Tolou, Statically Balanced Compliant Mechanisms for Micro-precision, Delft University of Technology, 2012.
[134] G. Chen, S. Zhang, Fully-compliant statically-balanced mechanisms without prestressing assembly: concepts and case studies, Mech. Sci. 2 (2) (2011) 169–174.
[135] S. de Paula Pellegrini, Neutrally Stable Vibration Energy Harvesting, 2012.
[136] S. Shahruz, Design of mechanical band-pass filters for energy scavenging, J. Sound Vib. 292 (3–5) (2006) 987–998.
[137] S. Roundy, et al., Improving power output for vibration-based energy scavengers, IEEE Pervasive Comput. 4 (1) (2005) 28–36.
[138] H. Xue, Y. Hu, Q.-M. Wang, Broadband piezoelectric energy harvesting devices using multiple bimorphs with different operating frequencies, IEEE Trans. Ultrason. Ferroelectr. Freq. Control 55 (9) (2008) 2104–2108.
[139] H. Farokhi, A. Gholipour, M.H. Ghayesh, Efficient broadband vibration energy harvesting using multiple piezoelectric bimorphs, J. Appl. Mech. 87 (4) (2020).
[140] G.-H. Feng, J.-C. Hung, Optimal FOM designed piezoelectric microgenerator with energy harvesting in a wide vibration bandwidth, in: 2007 2nd IEEE International Conference on Nano/Micro Engineered and Molecular Systems, IEEE, 2007.
[141] W. Al-Ashtari, et al., Enhanced energy harvesting using multiple piezoelectric elements: theory and experiments, Sens. Actuators A Phys. 200 (2013) 138–146.
[142] S. Dhote, H. Li, Z. Yang, Multi-frequency responses of compliant orthoplanar spring designs for widening the bandwidth of piezoelectric energy harvesters, Int. J. Mech. Sci. 157 (2019) 684–691.
[143] H. Zhang, K. Afzalul, Design and analysis of a connected broadband multi-piezoelectric-bimorph-beam energy harvester, IEEE Trans. Ultrason. Ferroelectr. Freq. Control 61 (6) (2014) 1016–1023.
[144] S. Li, et al., Bi-resonant structure with piezoelectric PVDF films for energy harvesting from random vibration sources at low frequency, Sens. Actuators A Phys. 247 (2016) 547–554.
[145] H. Deng, et al., Poly-stable energy harvesting based on synergetic multistable vibration, Commun. Phys. 2 (1) (2019) 21.
[146] Y. Hu, Y. Xu, A wideband vibration energy harvester based on a folded asymmetric gapped cantilever, Appl. Phys. Lett. 104 (5) (2014) 053902.
[147] X. Tang, L. Zuo, Enhanced vibration energy harvesting using dual-mass systems, J. Sound Vib. 330 (21) (2011) 5199–5209.
[148] Y. Tadesse, S. Zhang, S. Priya, Multimodal energy harvesting system: piezoelectric and electromagnetic, J. Intell. Mater. Syst. Struct. 20 (5) (2009) 625–632.
[149] L.J. Gong, et al., Harvesting vibration energy using two modal vibrations of a folded piezoelectric device, Appl. Phys. Lett. 107 (3) (2015) 033904.
[150] K. Moon, et al., A method of broadening the bandwidth by tuning the proof mass in a piezoelectric energy harvesting cantilever, Sens. Actuators A Phys. 276 (2018) 17–25.
[151] R. Chen, et al., Energy harvesting performance of a dandelion-like multi-directional piezoelectric vibration energy harvester, Sens. Actuators A Phys. 230 (2015) 1–8.
[152] S. Zhou, et al., Analytical and experimental investigation of flexible longitudinal zigzag structures for enhanced multi-directional energy harvesting, Smart Mater. Struct. 26 (3) (2017) 035008.
[153] G. Hu, et al., A twist piezoelectric beam for multi-directional energy harvesting, Smart Mater. Struct. 29 (11) (2020) 11LT01.
[154] J. Xu, J. Tang, Multi-directional energy harvesting by piezoelectric cantilever-pendulum with internal resonance, Appl. Phys. Lett. 107 (21) (2015) 213902.
[155] Z. Yang, J. Zu, Toward harvesting vibration energy from multiple directions by a nonlinear compressive-mode piezoelectric transducer, IEEE/ASME Trans. Mechatron. 21 (3) (2015) 1787–1791.
[156] B. Andò, et al., Two dimensional bistable vibration energy harvester, Procedia Eng. 47 (2012) 1061–1064.
[157] W.-J. Su, J. Zu, An innovative tri-directional broadband piezoelectric energy harvester, Appl. Phys. Lett. 103 (20) (2013) 203901.
[158] L. Gu, Low-frequency piezoelectric energy harvesting prototype suitable for the MEMS implementation, Microelectronics J. 42 (2) (2011) 277–282.
[159] M. Ferrari, et al., Impact-enhanced multi-beam piezoelectric converter for energy harvesting in autonomous sensors, Procedia Eng. 47 (2012) 418–421.
[160] H. Liu, et al., A scrape-through piezoelectric MEMS energy harvester with frequency broadband and up-conversion behaviors, Microsyst. Technol. 17 (12) (2011) 1747–1754.
[161] J. Zhang, L. Qin, A tunable frequency up-conversion wideband piezoelectric vibration energy harvester for low-frequency variable environment using a novel impact-and rope-driven hybrid mechanism, Appl. Energy 240 (2019) 26–34.
[162] Q. Tang, X. Li, A wide-band piezoelectric energy-harvester for high-efficiency power generation at low frequencies, in: 2013 Transducers & Eurosensors XXVII: The 17th International Conference on Solid-State Sensors, Actuators and Microsystems (TRANSDUCERS & EUROSENSORS XXVII), IEEE, 2013.
[163] Q. Tang, X. Li, Two-stage wideband energy harvester driven by multimode coupled vibration, IEEE/ASME Trans. Mechatron. 20 (1) (2014) 115–121.
[164] S. Chen, et al., A magnetic force induced frequency-up-conversion energy harvesting system., in: 2016 12th IEEE/ASME International Conference on Mechatronic and Embedded Systems and Applications (MESA), IEEE, 2016.
[165] A. Wickenheiser, E. Garcia, Broadband vibration-based energy harvesting improvement through frequency up-conversion by magnetic excitation, Smart Mater. Struct. 19 (6) (2010) 065020.
[166] T. Galchev, E.E. Aktakka, K. Najafi, A piezoelectric parametric frequency increased generator for harvesting low-frequency vibrations, J. Microelectromechanical Syst. 21 (6) (2012) 1311–1320.
[167] P. Panthongsy, et al., Fabrication and evaluation of energy harvesting floor using piezoelectric frequency up-converting mechanism, Sens. Actuators A Phys. 279 (2018) 321–330.
[168] B. Andò, et al., A nonlinear harvester to scavenge energy from rotational motion, in: 2019 IEEE International Instrumentation and Measurement Technology Conference (I2MTC), IEEE, 2019.
[169] B. Andò, et al., A low-threshold bistable device for energy scavenging from wideband mechanical vibrations, IEEE Trans. Instrum. Meas. (99) (2018) 1–11.
[170] S.-M. Jung, K.-S. Yun, Energy-harvesting device with mechanical frequency-up conversion mechanism for increased power efficiency and wideband operation, Appl. Phys. Lett. 96 (11) (2010) 111906.

[171] D. Han, K.-S. Yun, Piezoelectric energy harvester using mechanical frequency up conversion for operation at low-level accelerations and low-frequency vibration, Microsyst. Technol. 21 (8) (2015) 1669–1676.
[172] G.-W. Kim, J. Kim, Compliant bistable mechanism for low frequency vibration energy harvester inspired by auditory hair bundle structures, Smart Mater. Struct. 22 (1) (2012) 014005.
[173] N. Jackson, et al., Shock-induced aluminum nitride based MEMS energy harvester to power a leadless pacemaker, Sens. Actuators A Phys. 264 (2017) 212–218.
[174] Q. Tang, Y. Yang, X. Li, Bi-stable frequency up-conversion piezoelectric energy harvester driven by non-contact magnetic repulsion, Smart Mater. Struct. 20 (12) (2011) 125011.
[175] H.G. Yeo, et al., Strongly (001) oriented bimorph PZT film on metal foils grown by rf-sputtering for wrist-worn piezoelectric energy harvesters, Adv. Funct. Mater. 28 (36) (2018) 1801327.
[176] P. Pillatsch, E.M. Yeatman, A.S. Holmes, A piezoelectric frequency up-converting energy harvester with rotating proof mass for human body applications, Sens. Actuators A Phys. 206 (2014) 178–185.
[177] K. Fan, et al., Design and development of a multipurpose piezoelectric energy harvester, Energy Convers. Manage. 96 (2015) 430–439.
[178] K. Fan, et al., A nonlinear piezoelectric energy harvester for various mechanical motions, Appl. Phys. Lett. 106 (22) (2015) 223902.
[179] M. Hara, H. Kuwano, Lead-free (K, Na) NbO 3 impact-induced-Oscillation microenergy harvester, J. Microelectromechanical Syst. 24 (6) (2015) 1887–1895.
[180] D. Farhadi Machekposhti, J.L. Herder, N. Tolou, Frequency doubling in elastic mechanisms using buckling of microflexures, Appl. Phys. Lett. 115 (14) (2019) 143503.
[181] D. Farhadi Machekposhti, et al., Swiss watch featuring Dutch precision, Mikroniek: vakblad voor precisie-technologie 58 (5) (2018).
[182] J. Baker, S. Roundy, P. Wright, Alternative geometries for increasing power density in vibration energy scavenging for wireless sensor networks, 3rd International Energy Conversion Engineering Conference (2005).
[183] F. Goldschmidtboeing, P. Woias, Characterization of different beam shapes for piezoelectric energy harvesting, J. Micromech. Microeng. 18 (10) (2008) 104013.
[184] B. Montazer, U. Sarma, Design and optimization of quadrilateral shaped PVDF cantilever for efficient conversion of energy from ambient vibration, IEEE Sens. J. 18 (10) (2018) 3977–3988.
[185] N. Jackson, et al., Evaluation of low-acceleration MEMS piezoelectric energy harvesting devices, Microsyst. Technol. 20 (4–5) (2014) 671–680.
[186] X. Ma, et al., Efficient energy harvesting using piezoelectric compliant mechanisms: theory and experiment, J. Vib. Acoust. 138 (2) (2016) 021005.
[187] H.G. Yeo, et al., Efficient piezoelectric energy harvesters utilizing (001) textured bimorph PZT films on flexible metal foils, Adv. Funct. Mater. 26 (32) (2016) 5940–5946.
[188] Y. Zhang, C.-H. Lee, Piezoelectric energy harvesting pedal integrated with a compliant load amplifier, Adv. Mech. Eng. 11 (1) (2019), p. 1687814018820142.
[189] S. Wen, Q. Xu, Design of a novel piezoelectric energy harvester for scavenging energy from human walking., in: 2018 IEEE/ASME International Conference on Advanced Intelligent Mechatronics (AIM)., IEEE, 2018.
[190] J. Feenstra, J. Granstrom, H. Sodano, Energy harvesting through a backpack employing a mechanically amplified piezoelectric stack, Mech. Syst. Signal Process. 22 (3) (2008) 721–734.
[191] D.-X. Cao, et al., Design and performance enhancement of a force-amplified piezoelectric stack energy harvester under pressure fluctuations in hydraulic pipeline systems, Sens. Actuators A Phys. (2020) 112031.
[192] T.R. Shrout, S.J. Zhang, Lead-free piezoelectric ceramics: alternatives for PZT? J. Electroceramics 19 (1) (2007) 113–126.
[193] P. Panda, B. Sahoo, PZT to lead free piezo ceramics: a review, Ferroelectrics 474 (1) (2015) 128–143.
[194] T.M. Kamel, G. de With, Poling of hard ferroelectric PZT ceramics, J. Eur. Ceram. Soc. 28 (9) (2008) 1827–1838.
[195] T.M. Kamel, F. Kools, G. De With, Poling of soft piezoceramic PZT, J. Eur. Ceram. Soc. 27 (6) (2007) 2471–2479.
[196] A. Safari, M. Abazari, Lead-free piezoelectric ceramics and thin films, IEEE Trans. Ultrason. Ferroelectr. Freq. Control 57 (10) (2010) 2165–2176.
[197] Y. Saito, et al., Lead-free piezoceramics, Nature 432 (7013) (2004) 84–87.
[198] I. Kanno, et al., Power-generation performance of lead-free (K, Na) NbO3 piezoelectric thin-film energy harvesters, Sens. Actuators A Phys. 179 (2012) 132–136.
[199] I. Kanno, et al., Vibration energy harvesters of lead-free (K, Na) NbO3 piezoelectric thin films, Proc. PowerMEMS (2011) 110–113.
[200] Z.L. Wang, Zinc oxide nanostructures: growth, properties and applications, J. Phys. Condens. Matter 16 (25) (2004) R829.
[201] H. Bardaweel, et al., A Comparison of Piezoelectric Materials for MEMS Power Generation. In the Sixth International Workshop on Micro and Nanotechnology for Power Generation and Energy Conversion Applications, 2006.
[202] A. Tran, AlN Piezoelectric Films for Sensing and Actuation, 2014.
[203] K. Tonisch, et al., Piezoelectric properties of polycrystalline AlN thin films for MEMS application, Sens. Actuators A Phys. 132 (2) (2006) 658–663.
[204] N. Jackson, L. Keeney, A. Mathewson, Flexible-CMOS and biocompatible piezoelectric AlN material for MEMS applications, Smart Mater. Struct. 22 (11) (2013) 115033.
[205] N.G. Berg, T. Paskova, A. Ivanisevic, Tuning the biocompatibility of aluminum nitride, Mater. Lett. 189 (2017) 1–4.
[206] K. Karakaya, et al., The effect of the built-in stress level of AlN layers on the properties of piezoelectric vibration energy harvesters, J. Micromech. Microeng. 18 (10) (2008) 104012.
[207] A. Jain, et al., Dielectric and piezoelectric properties of PVDF/PZT composites: a review, Polym. Eng. Sci. 55 (7) (2015) 1589–1616.
[208] X. He, K. Yao, B.K. Gan, Phase transition and properties of a ferroelectric poly (vinylidene fluoride-hexafluoropropylene) copolymer, J. Appl. Phys. 97 (8) (2005) 084101.
[209] E.K. Akdogan, M. Allahverdi, A. Safari, Piezoelectric composites for sensor and actuator applications, IEEE Trans. Ultrason. Ferroelectr. Freq. Control 52 (5) (2005) 746–775.
[210] L. Ruan, et al., Properties and Applications of the β Phase Poly (vinylidene fluoride), Polymers 10 (3) (2018) 228.
[211] S. Priya, et al., A review on piezoelectric energy harvesting: materials, methods, and circuits, Energy Harvest. Syst. 4 (1) (2019) 3–39.
[212] K.-H. Cho, et al., Structure–performance relationships for cantilever-type piezoelectric energy harvesters, J. Appl. Phys. 115 (20) (2014) 204108.
[213] H. Palneedi, et al., A flexible, high-performance magnetoelectric heterostructure of (001) oriented pb (zr0. 52ti0. 48) o3 film grown on ni foil, APL Mater. 5 (9) (2017) 096111.
[214] J.H. Han, K.-I. Park, C.K. Jeong, Dual-structured flexible piezoelectric film energy harvesters for effectively integrated performance, Sensors 19 (6) (2019) 1444.
[215] J. Deng, et al., Topology optimization and fabrication of low frequency vibration energy harvesting microdevices, Smart Mater. Struct. 24 (2) (2014) 025005.
[216] C. Lan, et al., Equivalent impedance and power analysis of monostable piezoelectric energy harvesters, J. Intell. Mater. Syst. Struct. 31 (14) (2020) 1697–1715.
[217] Y. Liao, J. Liang, Unified modeling, analysis and comparison of piezoelectric vibration energy harvesters, Mech. Syst. Signal Process. 123 (2019) 403–425.
[218] D. Shen, Piezoelectric Energy Harvesting Devices for Low Frequency Vibration Applications, 2009.
[219] V.R. Challa, et al., A vibration energy harvesting device with bidirectional resonance frequency tunability, Smart Mater. Struct. 17 (1) (2008) 015035.
[220] D. Zhu, et al., A credit card sized self powered smart sensor node, Sens. Actuators A Phys. 169 (2) (2011) 317–325.
[221] A. Lei, et al., MEMS-based thick film PZT vibrational energy harvester., in: 2011 IEEE 24th International Conference on Micro Electro Mechanical Systems, IEEE, 2011.
[222] J.C. Park, J.Y. Park, Y.-P. Lee, Modeling and characterization of piezoelectric $ d_ {33} $-mode MEMS energy harvester, J. Microelectromechanical Syst. 19 (5) (2010) 1215–1222.
[223] H.-B. Fang, et al., Fabrication and performance of MEMS-based piezoelectric power generator for vibration energy harvesting, Microelectronics J. 37 (11) (2006) 1280–1284.
[224] B. Lee, et al., Piezoelectric MEMS generators fabricated with an aerosol deposition PZT thin film, J. Micromech. Microeng. 19 (6) (2009) 065014.
[225] D. Isarakorn, et al., The realization and performance of vibration energy harvesting MEMS devices based on an epitaxial piezoelectric thin film, Smart Mater. Struct. 20 (2) (2011) 025015.
[226] P. Muralt, et al., Vibration energy harvesting with PZT micro device, Procedia Chem. 1 (1) (2009) 1191–1194.
[227] K. Morimoto, et al., High-efficiency piezoelectric energy harvesters of c-axis-oriented epitaxial PZT films transferred onto stainless steel cantilevers, Sens. Actuators A Phys. 163 (1) (2010) 428–432.
[228] H. Durou, et al., Micromachined bulk PZT piezoelectric vibration harvester to improve effectiveness over low amplitude and low frequency vibrations, Proc. Power MEMS'10 (2010) 27–30.
[229] M. Hara, et al., Bulk micromachined energy harvesters employing (K, Na) NbO3 thin film, J. Micromech. Microeng. 23 (3) (2013) 035029.
[230] S.S. Won, et al., Lead-free Mn-doped (K0. 5, Na0. 5) NbO3 piezoelectric thin films for MEMS-based vibrational energy harvester applications, Appl. Phys. Lett. 108 (23) (2016) 232908.
[231] P. Wang, H. Du, ZnO thin film piezoelectric MEMS vibration energy harvesters with two piezoelectric elements for higher output performance, Rev. Sci. Instrum. 86 (7) (2015) 075002.
[232] K. Tao, et al., Piezoelectric ZnO thin films for 2DOF MEMS vibrational energy harvesting, Surf. Coat. Technol. 359 (2019) 289–295.
[233] R. Elfrink, et al., Vibration energy harvesting with aluminum nitride-based piezoelectric devices, J. Micromech. Microeng. 19 (9) (2009) 094005.
[234] T. Hirasawa, et al., Design and fabrication of piezoelectric aluminum nitride corrugated beam energy harvester, Proc. Power MEMS (2010) 211–214.
[235] R. Elfrink, et al., Vacuum-packaged piezoelectric vibration energy harvesters: damping contributions and autonomy for a wireless sensor system, J. Micromech. Microeng. 20 (10) (2010) 104001.
[236] M. Marzencki, Y. Ammar, S. Basrour, Integrated power harvesting system including a MEMS generator and a power management circuit, Sens. Actuators A Phys. 145 (2008) 363–370.

[237] R. Andosca, et al., Experimental and theoretical studies on MEMS piezoelectric vibrational energy harvesters with mass loading, Sens. Actuators A Phys. 178 (2012) 76–87.
[238] A.B.A. Dow, et al., Design, fabrication and testing of a piezoelectric energy microgenerator, Microsyst. Technol. 20 (4–5) (2014) 1035–1040.
[239] N. Jackson, et al., Influence of aluminum nitride crystal orientation on MEMS energy harvesting device performance, J. Micromech. Microeng. 23 (7) (2013) 075014.
[240] S. Kim, et al., P (VDF-TrFE) film on PDMS substrate for energy harvesting applications, Appl. Sci. 8 (2) (2018) 213.
[241] Z. Cao, J. Zhang, H. Kuwano, Vibration energy harvesting characterization of 1 cm2 Poly (vinylidene fluoride) generators in vacuum, J. Appl. Phys. 50 (9S2) (2011) 09ND15.
[242] J. Song, et al., Design optimization of PVDF-based piezoelectric energy harvesters, Heliyon 3 (9) (2017).

Biographies

Haitong Liang is currently a PhD student in Tyndall National Institute/School of Engineering and Architecture, University College Cork, under the supervision of Dr. Guangbo Hao and Dr. Oskar Z. Olszewski. His research topic is piezoelectric energy harvesting based on compliant mechanisms. He received his B.S. degree in Mechanical Engineering from Taiyuan University of Technology (2012) and the M.S. degree in Mechanical Engineering from Beihang University (2015). Before his doctoral study, he had 3-year experience in mechanical design as an engineer.

Dr. Guangbo Hao is a Senior Lecturer with University College Cork, Ireland. His research areas lie in design of compliant mechanisms and robotics and their applications in precision engineering, energy harvesting and biomedical devices. He obtained his PhD degree in Mechanical Engineering from Heriot-Watt University in 2011. He is a member of ASME and an elected member of the ASME Mechanisms and Robotics Committee. He is serving as the Editor-in-Chief of the IFToMM affiliated journal: Mechanical Sciences and the Associate Editor of ASME Journal of Mechanisms and Robotics. He has won some accolades including the 2017 and 2018 ASME Compliant Mechanisms Awards in a row. He has published over 140 peer-reviewed journal papers. More can be found from the website: https://sites.google.com/site/doctorghao/

Oskar Z. Olszewski received the B.Sc. degree in Electronics from the Gdynia Maritime Academy, Gdynia, Poland, in 2002, the M.Eng. degree in Electronic Engineering from the Cork Institute of Technology, Cork, Ireland, in 2004, and the PhD degree in Microelectronics from the University College Cork, Cork, Ireland, in 2010. He is a senior researcher at Tyndall National Institute, Cork, Ireland, where he is involved in research in the field of MEMS technology. His interests include device design and modelling, process development, and device characterization. In particular, he currently works on piezoelectric (AlN and AlScN) resonators and actuators for various MEMS applications.